Irradiation Test of Shielding Material for Fast Reactor JMTR-SH(I) (71M-84P)

March, 1976

POWER REACTOR AND NUCLEAR FUEL DEVELOPMENT CORPORATION

PNC TN951 76-05
Mar., 1976

Irradiation Test of Shielding Material for Fast Reactor

JMTR-SH(I) (71M-84P)

Kazuhisa Suzuki*, Sadamu Yamanouchi*, Satoshi Tani*, Akio Ichige*, Takeshi Naito*, Mamoru Harada*, Masahiko Ito*, Shoichi Osugi**, and Kenichi Shibata**

Abstract

The serpentine concrete in which two kinds of cement were used as a binder was irradiated in JMTR to the fast neutron fluence - 1.7×10^{19} n/cm^2 (E $>$ 1MeV) and thermal neutron fluence - 1.5×10^{20} n/cm^2. Average irradiation temperature was estimated to be 200 °C. Prior to the post-irradiation examination, effect of thermal history was investigated in out-of-pile test. The integrity of specimens were kept after irradiation.
From the results of thermal history examination and the post-irradiation examination, it was clearly noticed that the changes occurring in dimensions, weight and compressive strength were caused mainly by the thermal effect. The change in the Young's modulus seemed to be caused by the effect of both heating and neutron irradiation.
It was concluded that the ordinary portland cement with the serpentine concrete is better than that of almina cement.
This report was published in Japanese PNC's Report No. SN941 75-93, issued in Oct., 1975.

---

* Materials Monitoring Facility (MMF), Fuel and Material Division
** Present Address: No. 1 Test Sec., Takasago Laboratory, Mitsubishi Heavy Industries, Ltd.
*** Present Address: Atomic Equipment Sec., Yokohama Laboratory, Ishikawajima-Harima Industries Co., Ltd.

CONTENTS

Tables

Figures

Photographs

1. Introduction

High beam of fast neutrons leaked from the reactor vessel of the fast breeder reactor collides directly with the biological shielding concrete (ordinary concrete) and generates a large quantity of heat, if a special shielding is not provided around the vessel against such neutrons. The allowable temperature and temperature gradient for the biological shielding concrete are usually designed as 70 °C and 0.8 °C/mm respectively. In order to meet such conditions, shielding is required to be provided against neutrons between the reactor vessel and the biological shielding concrete. Effective shielding must be provided not only against neutrons but also γ -rays that leak from the reactor vessel.

The shielding material against neutrons should screen the neutrons and γ -rays and should be effectively bearable against elevated temperature.

Sodium used as coolant for the fast breeder reactor restricts the use of water near the reactor vessel. For such reasons, the graphite block[1)] has so far been used as the shielding material for the fast breeder reactor as in the case of the experimental fast breeder reactor, "JOYO".

The graphite block, however, poses a structural problem in the case of a large-sized prototype reactor or demonstration reactor. Furthermore, economical restriction arises from the unconsiderable quantity of graphite used. From the viewpoint of the shielding capability, thermal resistance, structural and economical restrictions, a new idea occurred to substitute for graphite a concrete (serpentine concrete) containing the aggregate of serpentine which contains a large amount of water in crystal.

As compared with graphite, serpentine concrete is better than

graphite in its shielding capacity against neutrons as shown in Fig. 1. (based on the results of the primary design for "MONJU"). However, in terms of thermal resistance, it is inferior to graphite. The applicable temperature range was between 200 and 250 °C in the case of prototype reactor "MONJU". No actual results of use for a long term at such elevated temperature must first be made clear. Thermal resistance has been examined in out-of-pile test and its practical use has become promissing to some extent.[2,3,4]

However, as regards the irradiation resistance which is required besides the thermal resistance, no confirmation has been made excepting a few reports.[5,6,7]

In the present examination, the serpentine concrete to be used in the prototype reactor, "MONJU", was irradiated for four cycles under the practical conditions for "MONJU", namely the fast neutron fluence - 2×10^{19} n/cm^2, temperature ranging between 200 and 250 °C, in the Japan Material Testing Reactor (JMTR) of the Japan Atomic Energy Research Institute in a period from November, 1973 to May, 1974.

Characteristics of concrete depend remarkably on temperature and, therefore, it is conceivable that the irradiation temperature affects greatly the results of the post-irradiation examination. In order to evaluate the effects of temperature separately from those of neutron irradiation, an out-of-pile test was conducted in the same manner as that of the post-irradiation examination, by giving the same thermal history as that received during irradiation, using specimens same in its lot and shape.

The cement used in the test was the ordinary portland cement and alumina cement. To compare these two kinds of cement was one of the objects of this report.

2. Materials

2.1 Cement

In the present test, two kinds of cement, ordinary portland cement and alumina cement were used. Chemical composition of the ordinary portland cement is shown in Table 1 and that of alumina cement in Table 2. The alumina cement used was of the 1st-stage containing less iron.

2.2 Aggregate

Ordinary cement is effective as a shield against γ -rays. Use of rock containing water in crystal as aggregate is more effective as a shield against neutrons. From a variety of rock containing water in crystal, serpentine was selected because of its high content of water in crystal and easy procurement in Japan.[8)]

Chemical composition of serpentine used in the test is shown in Table 3 and the distribution of particle size is also shown in Table 4.

2.3 Preparation of Test Specimens

Mixing rate of ordinary portland cement or alumina celement with serpentine and water is shown in Table 5, and a plate-shaped concrete specimen (mother material) of 30cm in length, 30cm in width and 5cm in thickness, was made* From this mother material, specimens for measuring Young's modulus (30 x 30 x 120 mm, long size specimen) and specimens for measuring compressive strength (30 x 30 x 60 mm, short size specimen) were made.

---

* The mother material was made in June, 1972.

3. Irradiation Capsule and Out-of-Pile Test Apparatus

3.1 Irradiation Capsule

The irradiation capsule is shown in Fig. 2. The capsule consisted of components such as external cylinder, thermal medium and spring. It contained 2 long size specimens and 2 short size specimens of the serpentine concrete of ordinary portland cement, 2 short size specimens of serpentine concrete of alumina cement.

Before assembling, the specimen was wrapped with aluminium foil and the specimen number was marked on it. Six pairs of Alumel-Chromel thermocouples were inserted. Two pairs were contacted in the thermal medium surrounding the specimen and four other pairs were placed in a gap between the specimen and the thermal medium. To measure the neutron fluence, Fe wires were placed as a flux monitor in the center and 250mm above and below the center of the reactor.

For the measurement of the pressure and radioactivity of gas which was discharged out from concrete during irradiation, a pressure gauge and a sampling tank were connected to the capsule as additional apparatus. The outline of this apparatus is shown in Fig. 3.

3.2 Out-of-Pile Test Device

This device is designed to give thermal history to the concrete specimen, and consists of a stainless steel specimen vessel, pressure gauge, He gas inlet and exhaust port. The specimen vessel alone is placed in the electric furnace. Fig. 4 shows the outlines of the device. The Alumel-Chromel thermocouple is placed around the central area of the specimen vessel to measure the specimen temperature. Two pairs of device are provided, one for serpentine concrete of ordinary portland cement and the other for the same concrete of alumina cement.

4. Irradiation and Out-of-Pile Test

4.1 Irradiation

The capsule was irradiated for four cycles (approximately 50 days) at the irradiating hole I-3 of the Japan Material Testing Reactor (JMTR) as shown in Fig. 5. The operation history of JMTR during the test is shown in Fig. 6 and the thermal cycle records indicated by the thermocouple during operation are shown in Fig. 7.

Fig. 8 shows the irradiation conditions (estimated values). Here, the temperature at the center of the specimen was estimated from the results of the calculation of γ -ray heating (see Appendix-IV) and the temperature measured by the thermocouple. The internal gas pressure and gas activity produced in the specimen during irradiation were measured. No radionuclide was detected.

4.2 Out-of-Pile Test

To make sure of the thermal effect on the serpentine concrete, an out-of-pile thermal cycle test was made using the specimen from the same lot of irradiation samples. Taking into account the irradiation temperature, test was conducted at 200 $^{\circ}$C. Thermal history was given in conformity to the operation history in JMTR.

The thermal history given to specimens is shown in Fig. 9. In this connection, Group A shows the result of the test before giving thermal history, Group F the result of test after the specimen was kept at room temperature for the period of time required to provide thermal history and Group B-E, the results of test after giving thermal history for the period shown in the Fig. 9.

5. Measuring Method

Visual inspection was done by eyes for specimens for out-of-pile test and by remotely operated periscope for the post-irradiation examination.

In measuring dimensions, vernier calipers were used for specimens for out-of-pile test and the photoelectric micrometer (measuring accuracy, $\pm 5\,\mu$) fitted with Nikon LS-5 type universal projector was used for specimens for post-irradiation examination.

In the case of long size specimen, measurement on 3 points in X, Y and axial directions and length was measured. In the case of short size specimen, measurement on 2 points in X and Y directions and length were measured.

Weight of specimens both in use for out-of-pile test and post-irradiation examination was measured by the automated chemical balance. Young's modulus was measured using Somiya's elastic modulus measuring device. By this device the primary longitudinal resonance vibration frequency formed in the square-column was measured and Young's modulus was calculated from the following formula.

Young's modulus, $E = C.W.f^2 \quad (Kg/cm^2)$

where, $C = 408 \times 10^{-5} \frac{L}{A} \quad (s^2/cm^2)$

W = Weight of specimen (g)

f = Primary longitudinal resonance vibration frequency

L = Length of specimen (cm)

A = Sectional area of specimen (cm^2)

Fig. 10 shows an outline of the device. The compressive strength test was made in accordance with test conditions based on JIS-A-1108, using tensile tester of Instron Corp. (max. testing load, 10 tons).

6. Test Results and Considerations

6-1. Visual Inspection

Photos. 1 and 2 show general views of unirradiated specimens, Photo. 3 shows general view of the irradiated specimens. Any crack and break with visual change were not observed on the irradiated specimens and difference was not found compared with unirradiated specimens. However, surface color change was observed on the serpentine concrete of ordinary portland cement (abbreviated as PS). This change was also observed on specimens provided with thermal history. Therefore, the cause of such change was considered to be the elevated temperature due to γ-ray heating and not the neutron irradiation.

In the case of the serpentine concrete of alumina cement (abbreviated as AS), no such color change was observed.

6-2 Internal Gas Pressure Measurement of Capsule

Internal gas pressure was measured during irradiation and heating (out-of-pile test) using Bludon tube. The results are shown in Figs. 11 and 12.

Radioactivity of gas generated during irradiation was measured, but no radionuclide was found. As the result of out-of-pile test, it was ascertained that difference of weight between before and after heating serpentine concrete. Weight loss was observed in irradiated specimens (mentioned later), and the increase of internal pressure in the capsule during irradiation may be caused by moisture discharged from the specimen.

6.3 Measurement of Dimensions

The results of dimensional measurement (length only) in the thermal history test and post-irradiation examination are shown in Table 6 and dimensional changes in Fig. 13. Contraction was observed on the specimens provided with thermal history and those kept at the room temperature. No difference between AS serpentine concrete and PS serpentine concrete was found. Contraction was observed in some of irradiated specimens and swelling in some others. In the case of the long size specimen, a mark was put at a central part for measurement. This may have resulted in a larger error as compared with that of the short size specimen.

Dubrovskii, et al.[5] irradiated the sandstone concrete (ordinary cement used) up to the fast neutron fluene - 1.7×10^{19} n/cm^2 ($E \geq 0.8$ MeV) and observed swelling (dimensional change) to an extent of 6 %. In the case of the serpentine concrete (ordinary cement used), irradiation was performed to a maximum of 1.7×10^{21} n/cm^2 at 350 °C and observed 1 % swelling.

Elleuch, et al.[7] irradiated serpentine concrete (alumina cement used) to a maximum of 10^{20} n/cm^2 ($E > 1$MeV), between 150 and 200 °C and observed about 0.25 % swelling at 2×10^{19} n/cm^2 and about 0.7 % swelling at 9×10^{19} n/cm^2. They also irradiated the serpentine in use for the aggregate and observed about 0.25 % swelling at 2×10^{19} n/cm^2 and about 0.6 % swelling at 9×10^{19} n/cm^2 respectively.

From the foregoing, it was concluded that the swelling of the serpentine concrete is caused by the property of its aggregate, namely the serpentine.

These results and results of this work are plotted against the fast neutron fluence in Fig. 14. From this Fig., it seems that swelling

begins at the fast neutron fluence 10^{19} n/cm^2 and contraction occurs when it is lowered therefrom.

The serpentine concrete contracts when thermal history is given.[3] On the other hand, the serpentine concrete swells after irradiation. Irradiation data for 10^{18} n/cm^2 (E $\geq$ 1MeV) are not available and accordingly it cannot be asserted, but at the initial stage (10^{19} n/cm^2 >), the thermal effect which causes contraction may be greater than the irradiation effect and when fluence exceeds 10^{19} n/cm^2, the irradiation effect becomes greater than thermal effect and swelling occurs. The fluence for the occurrence of such reversion seems to be about 10^{19} n/cm^2 (E > 1MeV).

6.4 Measurement of Weight

The results of thermal cycle test and post-irradiation test are shown in Table 7 and Fig. 15. In the case of the specimen provided with thermal cycle, weight decrease of 5 to 6 % was detected. It was about 6 % and 3 % respectively with the PS serpentine concrete and AS serpentine concrete after irradiation. As the results of thermal cycle test, it was clarified that weight reduction is caused by the desorption of moisture absorbed in the specimen. The quantity of the absorbed moisture affects the rate of weight reduction.

This weight reduction is closely related to the dimensional change and this correlation can be clearly observed when heat treating temperature is lower than 300 °C. Relations between dimensional change and weight change are shown in Fig. 16. In the case of specimen provided with thermal history, values agree well with those in the literature.[3,8] On the contrary, in the case of irradiated specimens, values of weight change and dimensional change are dislocated from

the respective curves. This may be attributed to the effect of irradiation.

6.5 Measurement of Young's Modulus

The results of thermal cycle test and post-irradiation test are shown in Table 8 and Fig. 17 (Young's Modulus Change). As regards the PS serpentine concrete provided with thermal history, AS serpentine concrete and irradiated specimen (limited to PS serpentine concrete), reduction of Young's modulus was observed to the extent of 11 %, 18 % and 30 % to 40 % respectively. The Young's modulus and weight change are reported to be closely correlated.[10] Relations between changes in Young's modulus and weight are shown in Fig. 18. Such correlation is observed comparatively clear in the case of the specimens provided with thermal history but no such correlation is found in the case of irradiated specimens. This may be attributed not only to the irradiation effect but also to the γ -ray heating effect.

Elleuch, et al.[7] have reported that they irradiated the serpentine concrete, serpentine and alumina cement paste to the fluence of 2×10^{19} n/cm^2 ($E > 1$MeV) at irradiation temperature between 150 and 200 $^{\circ}$C and observed such reduction to the extent of 20 %, 33% and 10 % respectively. The report noticed that as the results of the thermal cycle test on the serpentines sampled from the same lot of the irradiated specimens, about 10 % reduction was observed with the serpentine concrete, about 10 % reduction with the alumina cement paste and almost no reduction occurred with the serpentine. Accordingly, changes of Young's modulus that occurred in the specimens provided with thermal history may be regarded as such change

occurring in the cement.

The change in Young's modulus of the irradiated specimens is considered as the combined effect of such change of the cement plus that of the serpentine. This may be the reason why the reduction is more remarkable in the case of the irradiated specimens than the specimens provided with thermal history.

6.6 Compression Test

The results of the thermal cycle test and the results of post-irradiation examination are given in Table 9 and Fig. 19. After the compression test, ruptured state of specimens was observed and evaluation was limited to the sand-glass-shaped breaking only. Ruptured state of the materials provided with thermal history and irradiated specimens are shown in Photo. 4. In the case of PS serpentine concrete provided with thermal history, the strength seems to be reduced once but turns to be increased again. However, no such trend as in the PS serpentine concrete is observed in the case of AS serpentine concrete of which reduced strength seems to be kept at a constant value. In the case of specimens provided with thermal history, the compressive strength becomes lower with the alumina cement which is used at higher temperature. This fact was confirmed by Yamamura, et al.[8], but its exact reason has not yet been clarified.

On the irradiated specimens, little difference of strength is observed from the specimens provided with thermal history in the case of PS serpentine concrete, but in the case of AS serpentine concrete, the compressive strength was observed to be reduced to an extent of 1/3 as compared with that of unirradiated material.

Such extent of reduction was observed in compressive strength even with the specimens provided with thermal history.

According to Elleuch, et al.[7], compressive strength increases by irradiation. Therefore, the reduction in compressive strength after irradiation is attributed to the property of cement.

From the foregoing, radiation damage in alumina cement is thought to be greater than the ordinary portland cement when irradiated at about 200 °C.

7. Conclusion

The results of thermal cycle test and post-irradiation test are summarized as follows.

(1) The integrity of specimen is retained after irradiation and both PS and AS serpentine concrete can be used at least up to 1.7×10^{19} n/cm^2 ($E > 1MeV$).

(2) Dimensional contraction occurs in materials provided with thermal cycles. In some of the irradiated specimens, such contraction was observed but swelling was also found in some others. It is considered that, under irradiation up to 10^{19} n/cm^2 ($E > 1MeV$), specimens are contracted because of the thermal effect and swelling caused by neutron irradiation occurs when the fluence exceeds the above value.

(3) Young's modulus is observed to be reduced by 10 to 20 % in the case of materials provided with thermal cycles and 30 to 40 % with the irradiated specimens. Difference between the AS serpentine concrete and PS serpentine concrete is considered to be caused by the reduction of weight (reduction of moisture).

(4) The reduction rate of compressive strength is lower in PS serpentine concrete than in AS serpentine concrete. The similar trend can be seen in the irradiated specimens. The reduction rate is remarkably high in the case of AS serpentine concrete.

From these conclusions, the serpentine concrete of ordinary portland cement is preferred to the serpentine concrete of alumina cement when used at about 200 °C.

REFERENCE

1)* Application for Approval of the Design and Construction Method of Experimental Fast Reactor "JOYO" of the Power Reactor and Nuclear Fuel Development Corporation.

2)* Yamamura, et al., J230-71-01 (1971)

3)* Yamamura, et al., J230-73-02 (1973)

4)* Ishii, et al., J230-74-01 (1974)

5) V.B. Dubrovskii, et al., Atom. Ener. (USSR) Vol. 23, No. 4 (1964)

6) V.B. Dubrovskii, et al., Atom. Ener. (USSR) Vol. 29, No. 11 (1970)

7) M.F. Elleuch, et al., A/CONF49/P1613 (1971)

8)* Yamamura, et al., J230-72-01 (1972)

9)* Ishii, et al., SJ230-75-01 (1975)

10)* Uematsu, et al., Concrete Journal Vol. 12, No. 6 (1974)

* marks are issued in Japanese.

Table 1 Chemical Composition of Portland Cement

(%)

Igloss	Insol	SiO_2	Al_2O_3	Fe_2O_3	CaO	MgO	SO_3	Total
0.5	0.5	22.3	5.0	2.9	64.5	1.3	2.0	99.0

Table 2 Chemical Composition of Alumina Cement

(%)

Al_2O_3	Fe_2O_3	CaO	Total
55.0	2.6	37.4	100

Table 3 Chemical Composition of Serpentine

(%)

SiO_2	Al_2O_3	Fe_2O_3	FeO	MgO	CaO	Na_2O	K_2O	$H_2O(+)$	$H_2O(-)$	TiO_2	MnO	CO_2	Total
37.6	3.4	5.2	2.0	33.4	4.8	1.1	0.1	9.4	0.9	0.1	0.1	1.7	99.8

Table 4 Particle Size of Serpentine

(%)

5 ~ 2.5 mm	2.5 ~ 1.2	1.2 ~ 0.6	0.6 ~ 0.3	0.3~0.15	0.15 >
12	23	26	18	11	10

Table 5 Mixing Rate

Composition / Sample	Cement	Serpentine	Water
PS	15.5	76.5	8.0
AS	15.5	76.5	8.0

Table 6 Dimension of Serpentine Concrete

〔mm〕

Specimen	Thermal Cycle					Irradiation		Reference	
	0	196 hr	430 hr	857 hr	1185 hr	Unirra.	Postirra.	0	1185 hr
PS	120.10	120.00	120.00	119.85	119.90	120.20	120.14	119.90	119.75
	120.10	120.00	120.00	120.00	119.95	119.60	119.32	119.90	119.55
	119.40	119.35	119.35	119.35	119.40	60.10	60.17	120.10	119.90
	119.80	119.75	119.75	119.75	119.70	60.10	60.22	120.10	119.95
AS	120.15	120.00	120.10	120.10	120.00	59.90	59.92	120.30	120.30
	120.45	120.35	120.40	120.35	120.30	60.00	59.93	120.25	120.25
	120.10	119.95	120.00	120.00	120.00	—	—	119.95	119.90
	120.40	120.35	120.40	120.35	120.30	—	—	120.55	120.45

Table 7 Weight of Serpentine Concrete

〔g〕

Specimen	Thermal Cycle					Irradiation		Reference	
	0	196 hr	430 hr	875 hr	1185 hr	Unirra.	Postirra.	0	1185 hr
PS	229.0	218.7	218.8	217.9	217.2	229.4	215.1	230.0	228.2
	228.9	219.1	218.7	218.1	217.3	227.9	213.6	227.2	225.5
	227.9	217.1	216.9	216.7	216.0	115.4	108.9	229.7	227.8
	226.7	216.0	215.9	215.7	215.2	116.0	108.6	225.3	223.9
AS	226.8	213.8	213.9	213.0	212.7	114.2	110.1	223.4	222.3
	222.8	210.7	210.9	212.0	209.6	110.2	107.9	226.0	224.6
	221.4	208.8	208.9	208.5	208.1	—	—	225.9	224.7
	225.4	212.8	212.9	212.6	212.1	—	—	226.2	225.1

Table 8 Young's Modulus of Serpentine Concrete

〔Kg/cm²〕

Specimen	Thermal Cycle					Irradiation		Reference	
	0	196 hr	430 hr	875 hr	1185 hr	Unirra.	Postirra.	0	1185 hr
PS	2.35×10^5	2.30×10^5	2.06×10^5	2.08×10^5	2.08×10^5	2.45×10^5	1.51×10^5	2.48×10^5	2.51×10^5
	2.50	2.11	2.22	2.33	2.26	2.59	1.79	2.44	2.44
	2.51	2.12	2.30	2.30	2.28	—	—	2.39	2.39
	2.34	2.08	2.04	2.05	2.04	—	—	2.51	2.42
AS	2.31	1.54	1.82	1.80	1.78	—	—	2.30	2.36
	2.28	1.96	1.96	1.95	1.92	—	—	2.43	2.50
	2.22	1.88	1.86	1.83	1.83	—	—	2.39	2.44
	2.32	1.98	1.93	1.94	1.93	—	—	2.45	2.50

Table 9 Compressive Strength of Serpentine Concrete

〔Kg/cm²〕

Specimen	Thermal Cycle					Irradiation	
	0	196 hr	430hr	857hr	1185hr	Pre—	Post—
PS	486.1	420.1	361.4	494.2	495.8	—	460.6
	583.6	563.9	403.8	431.8	446.5	—	409.4
	—	546.0	481.6	434.7	560.6	—	—
AS	617.9	356.0	412.6	339.4	203.7	—	202.5
	559.8	369.0	367.4	314.9	380.8	—	215.1
	501.9	342.0	346.5	237.6	388.3	—	—

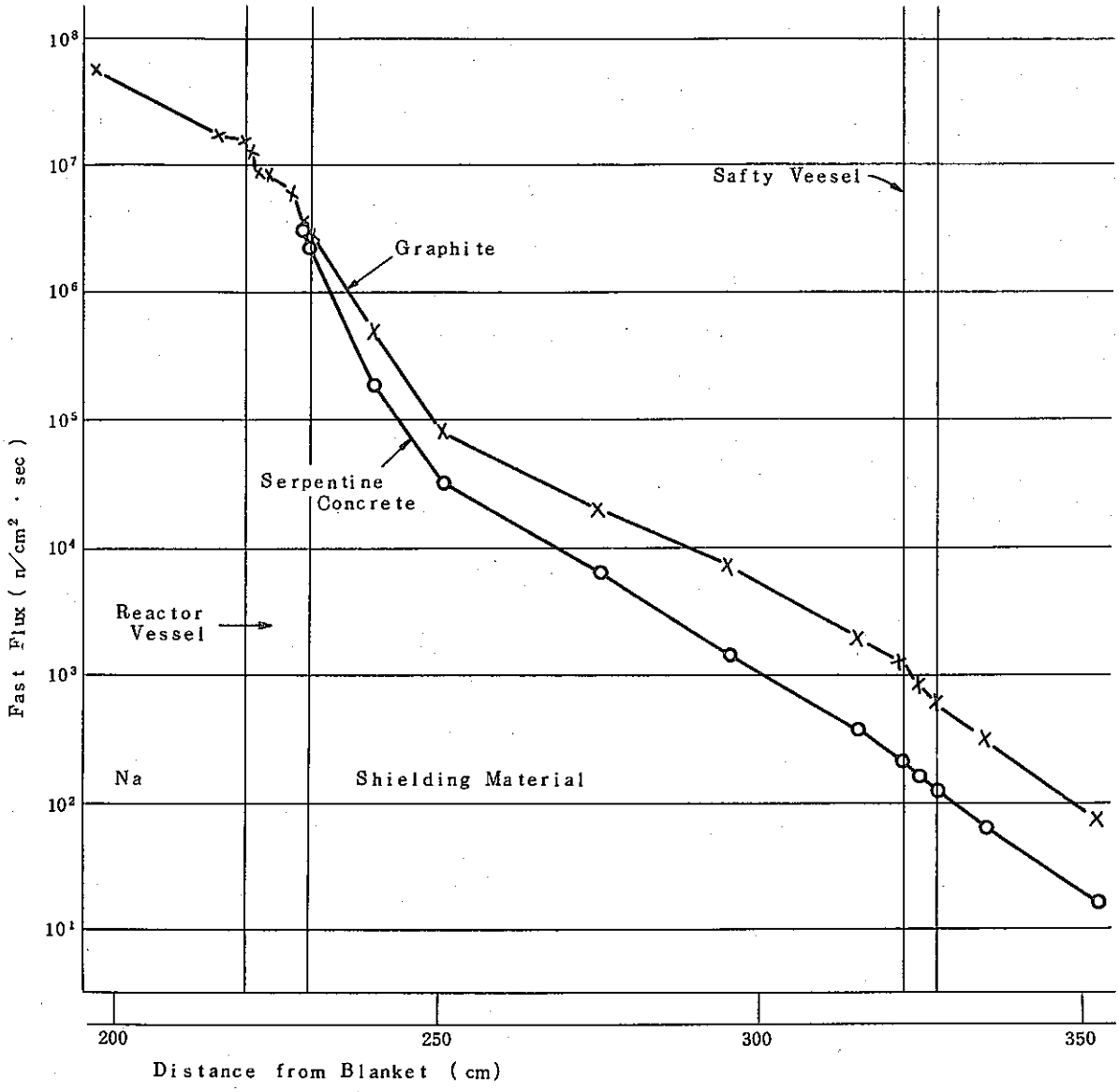

Fig. 1 Shield Effect of Serpentine Concrete and Graphite

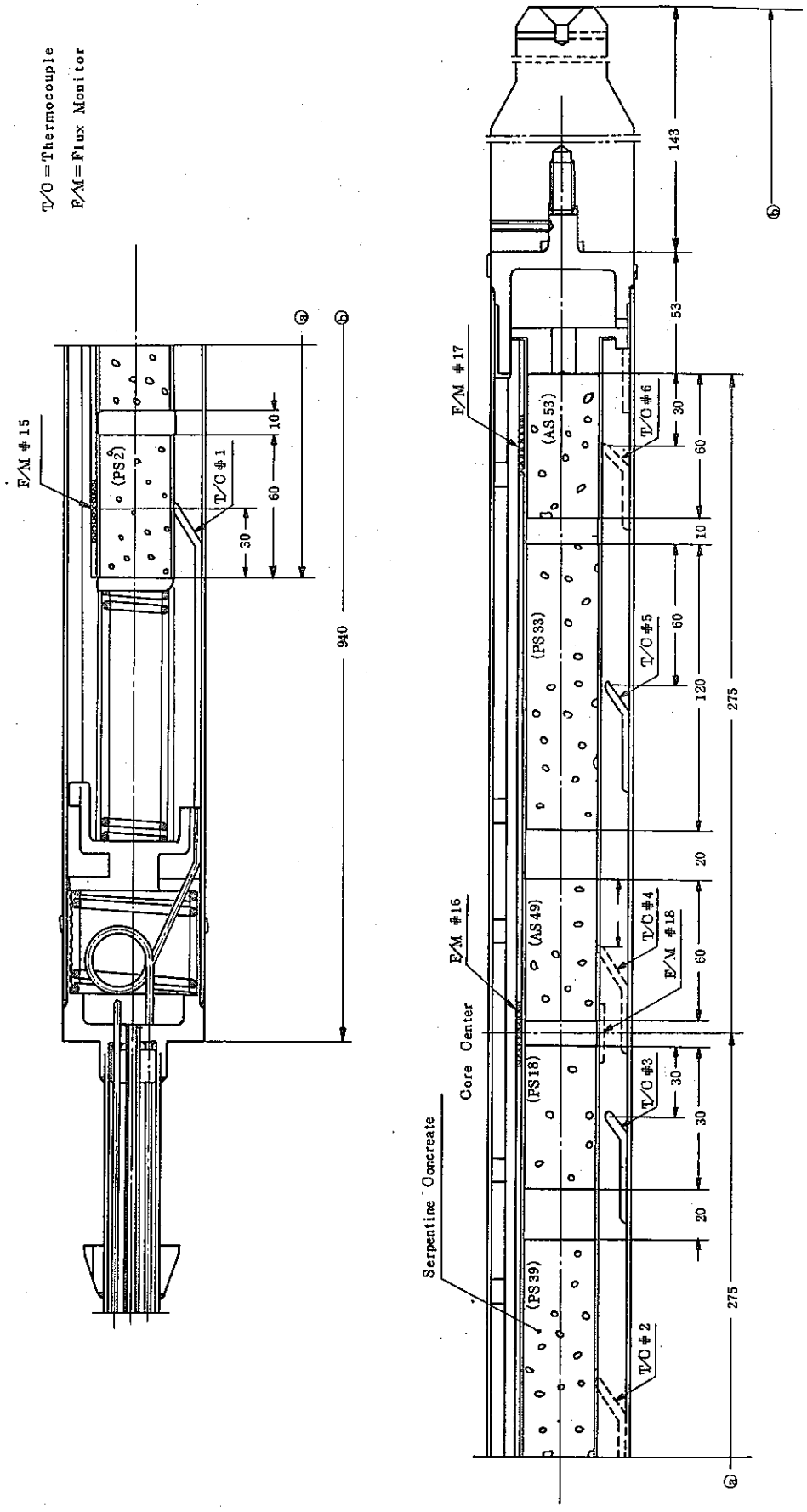

Fig. 2 Irradiation Capsule for JMTR-SH(I) Experiment

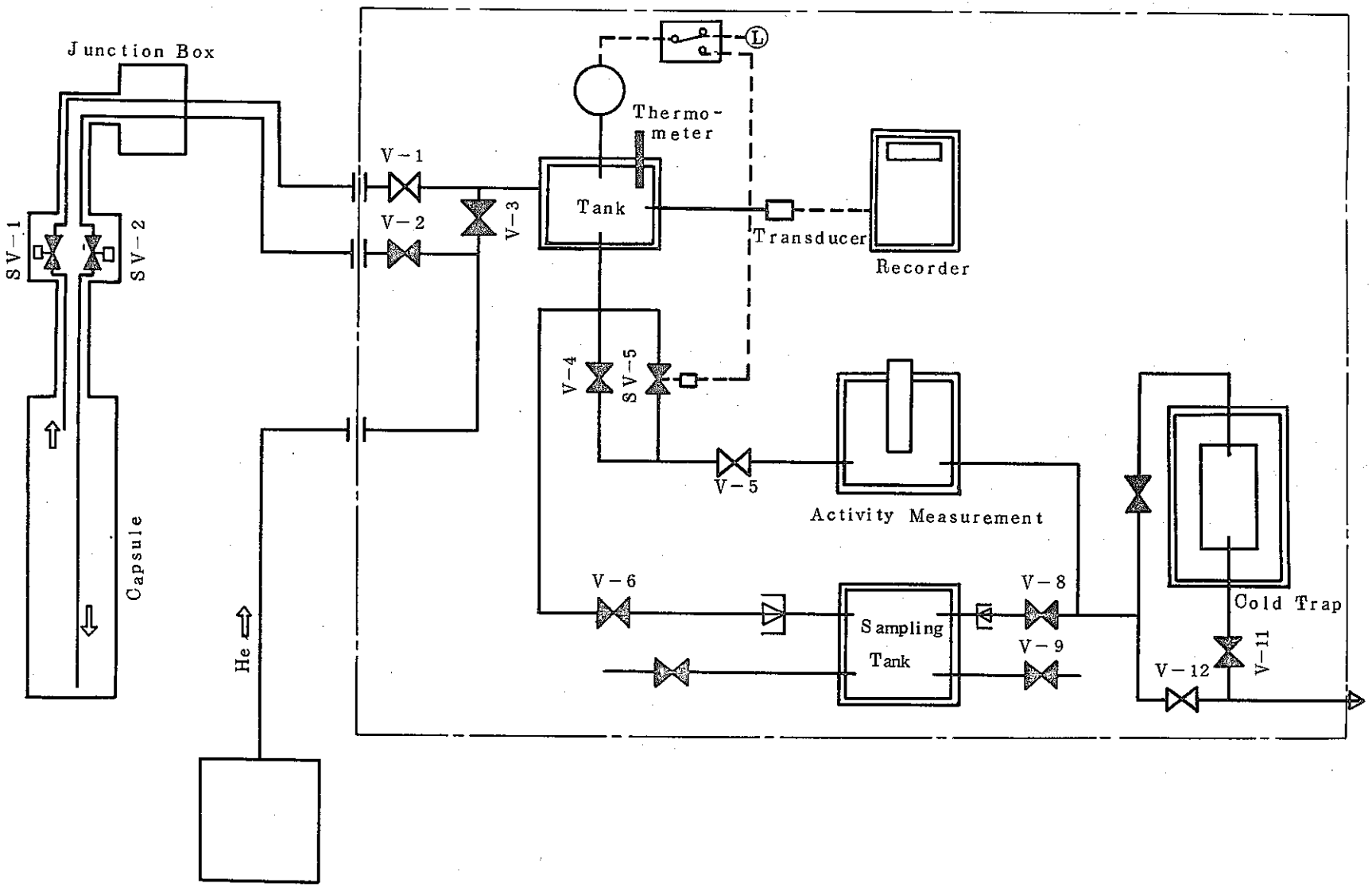

Fig. 3 Irradiation Apparatus for JMTR-SH(I)

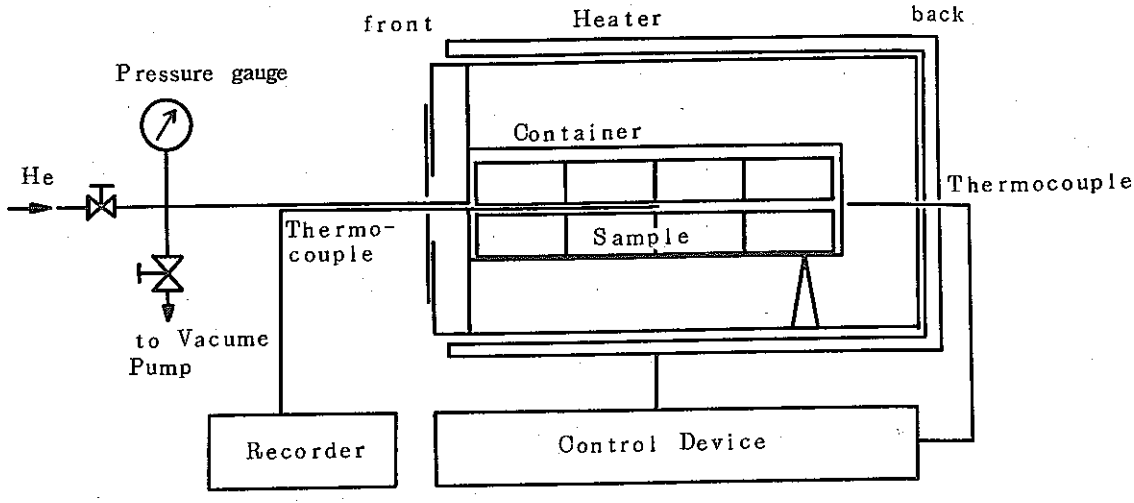

(1) Sectional Diagram of Apparatus

(a) Upper Row

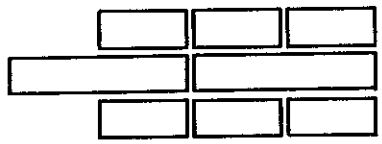

(b) Lower Row

(2) Specimen Arrangement in Container

Fig. 4 Apparatus for out-of-pile Test

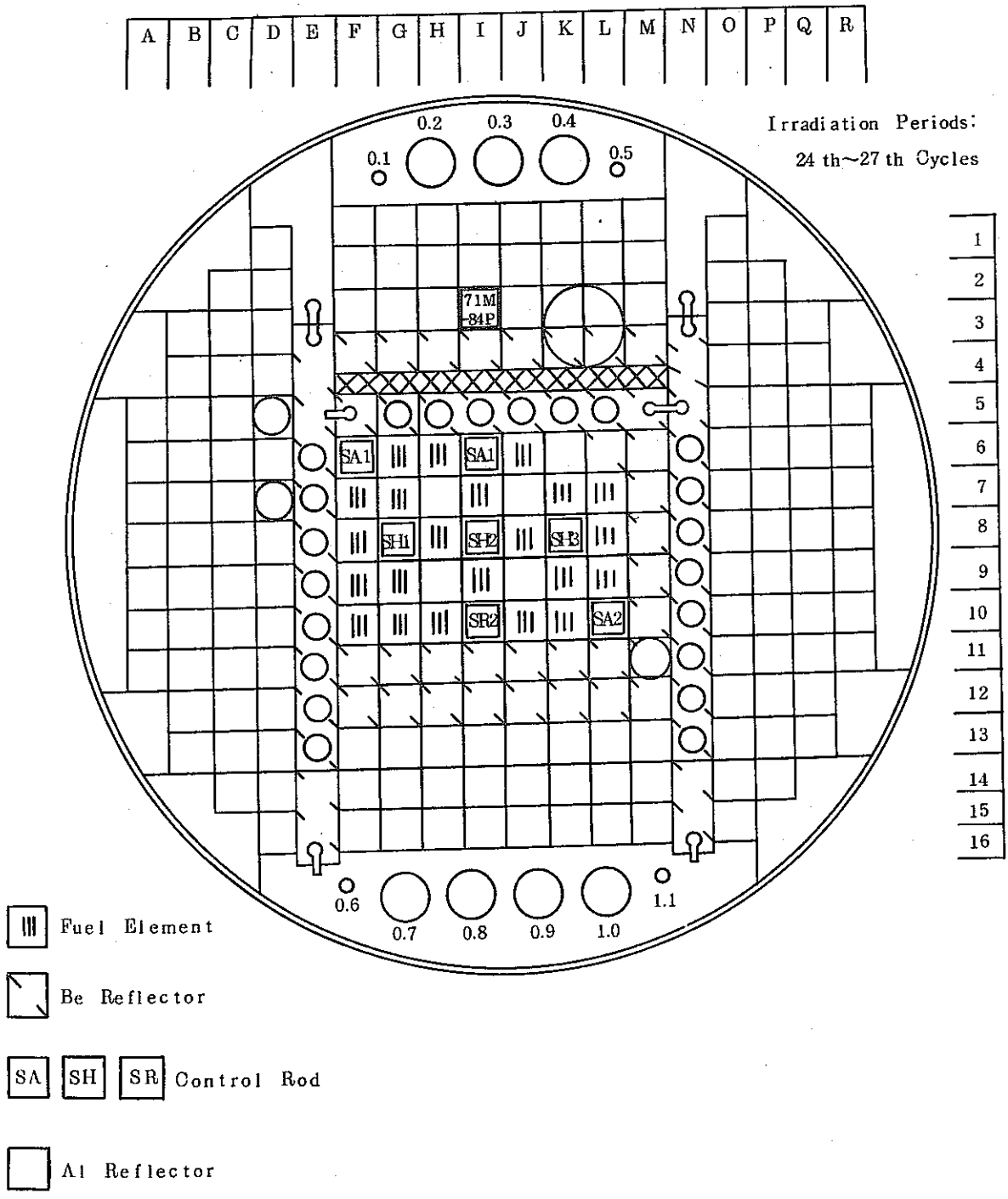

Fig. 5 Irradiation Position in JMTR Core

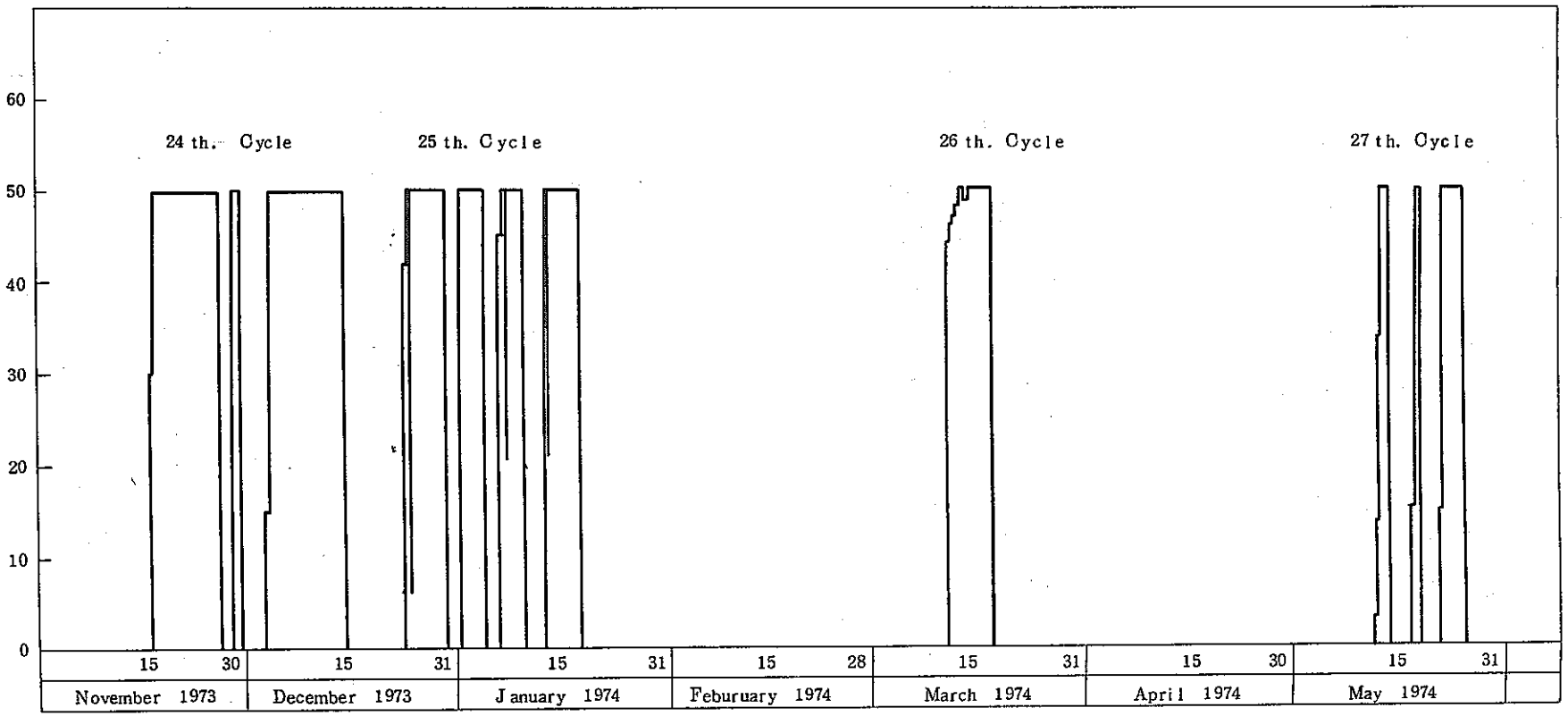

Fig. 6 Reactor Operation History

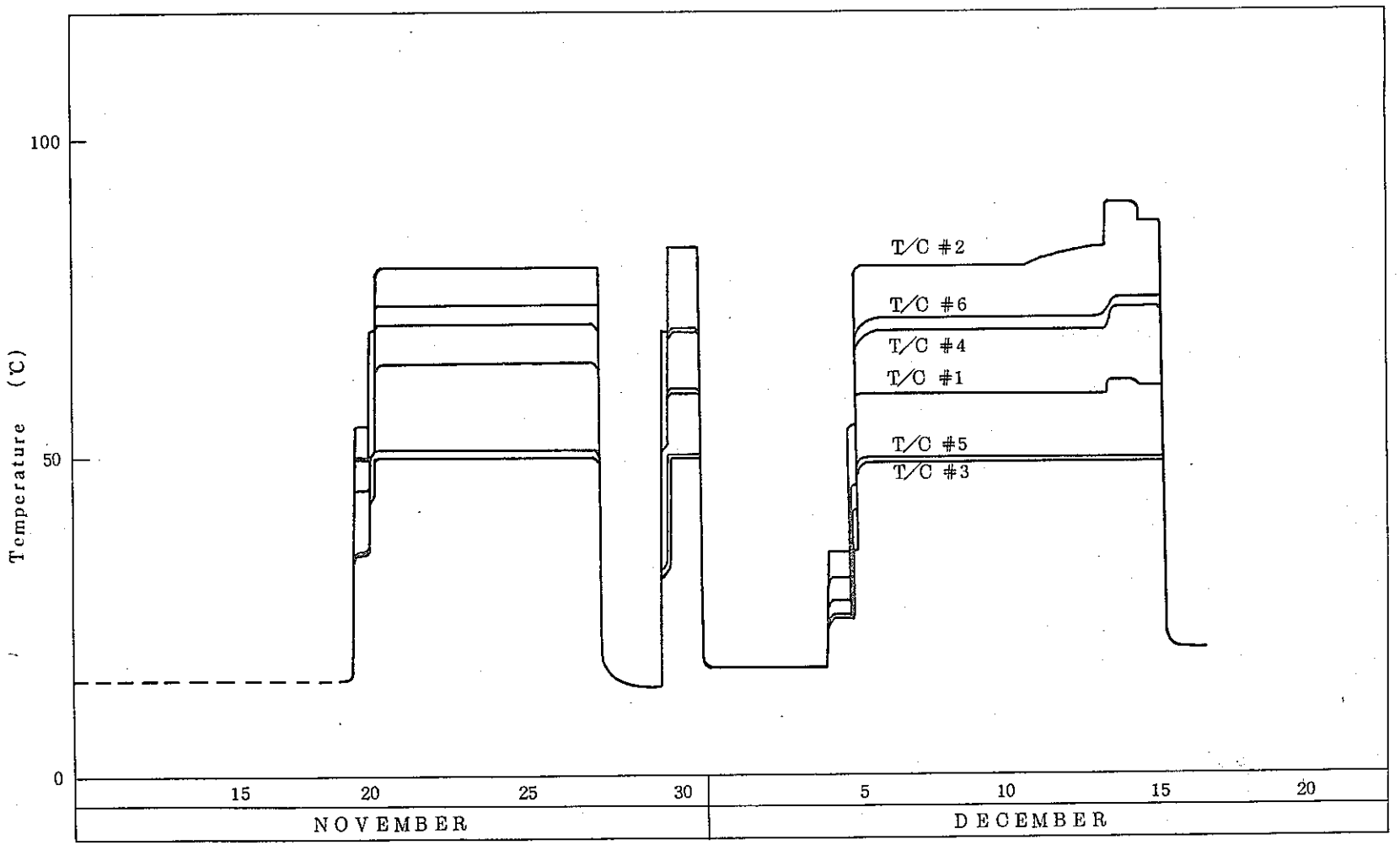

Fig. 7 Thermal History of JMTR 24th Cycle

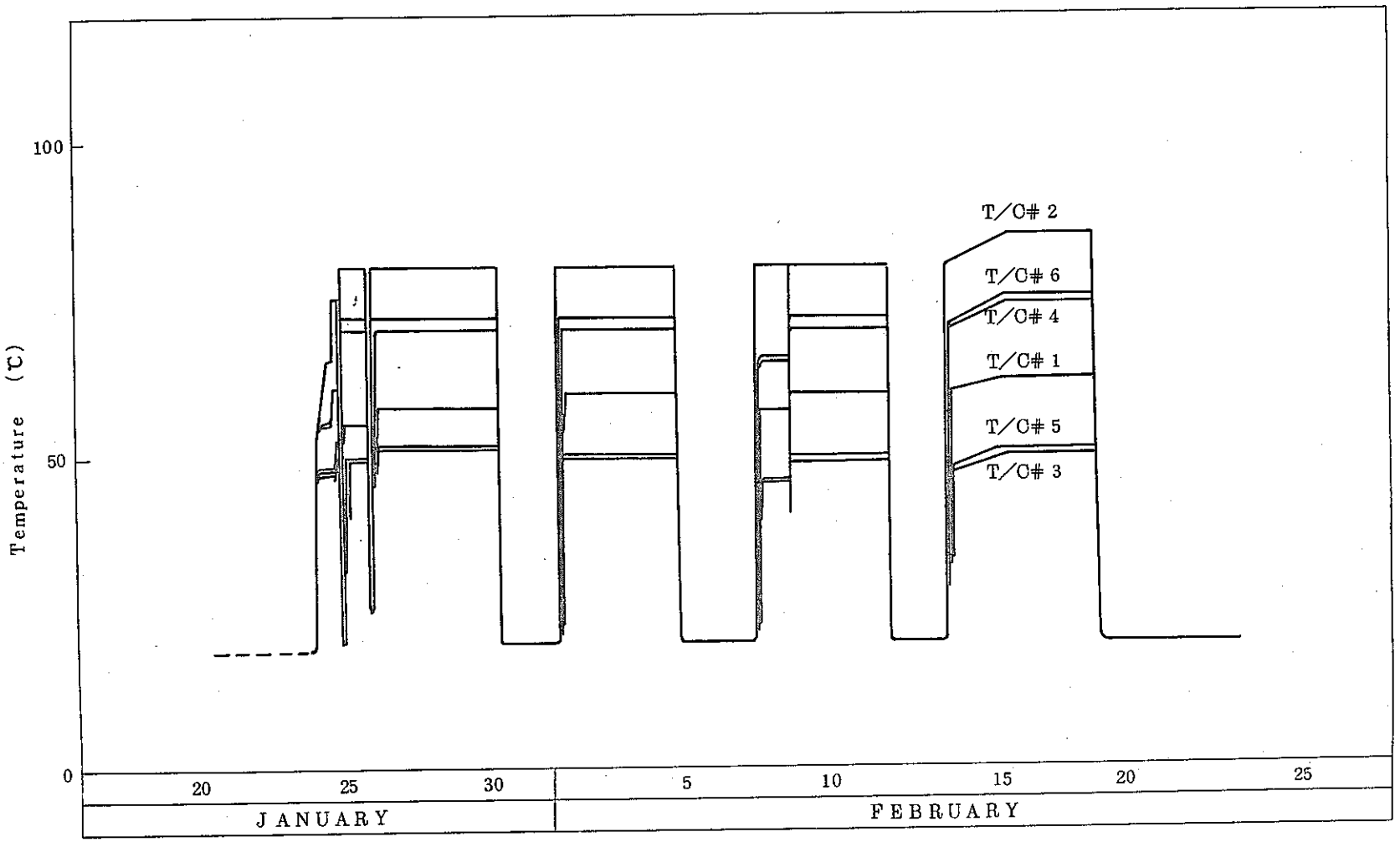

Fig. 7 Thermal History of JMTR 25th Cycle (Continued)

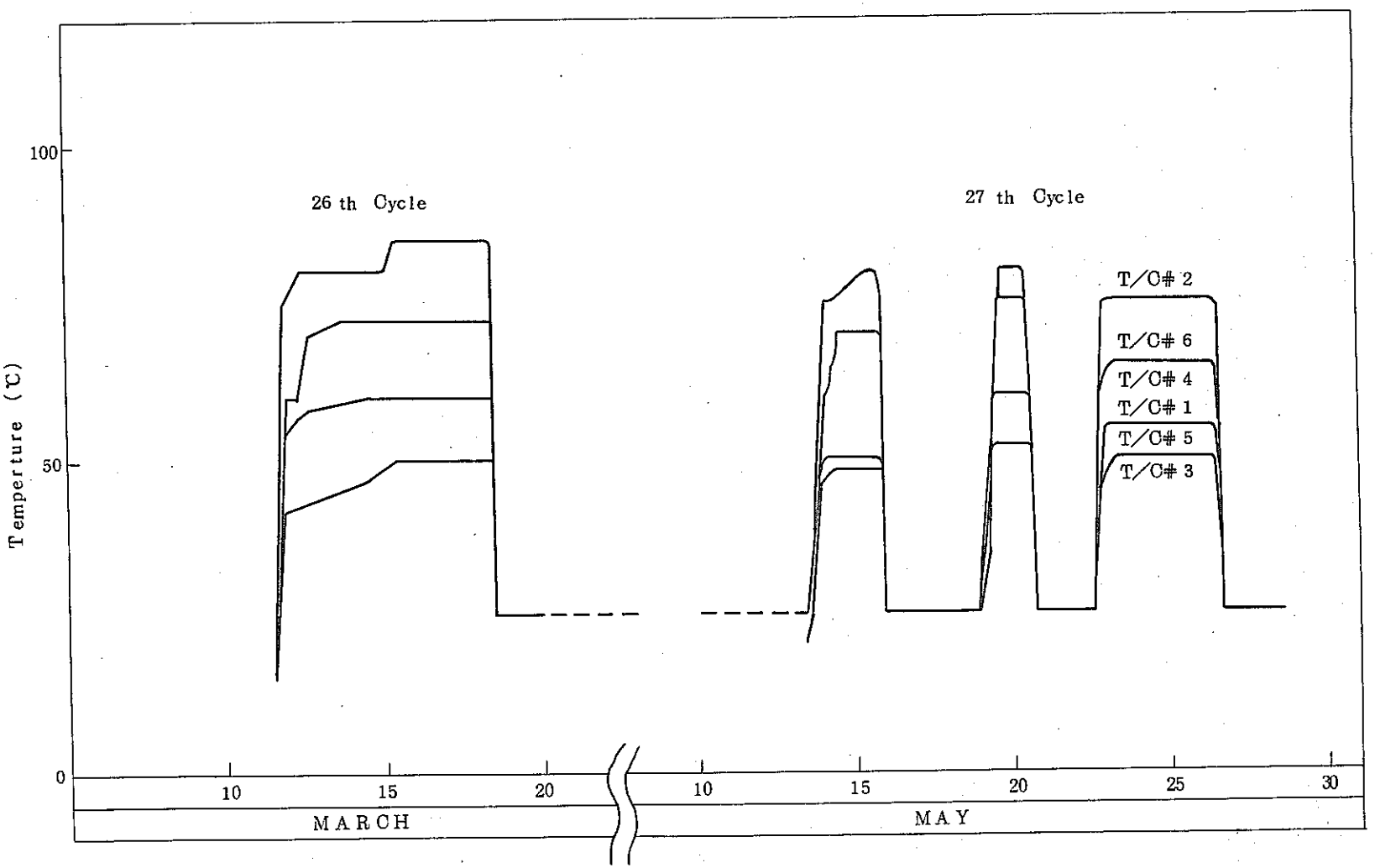

Fig. 7 Thermal History of JMTR 26th and 27th Cycles (Continued)

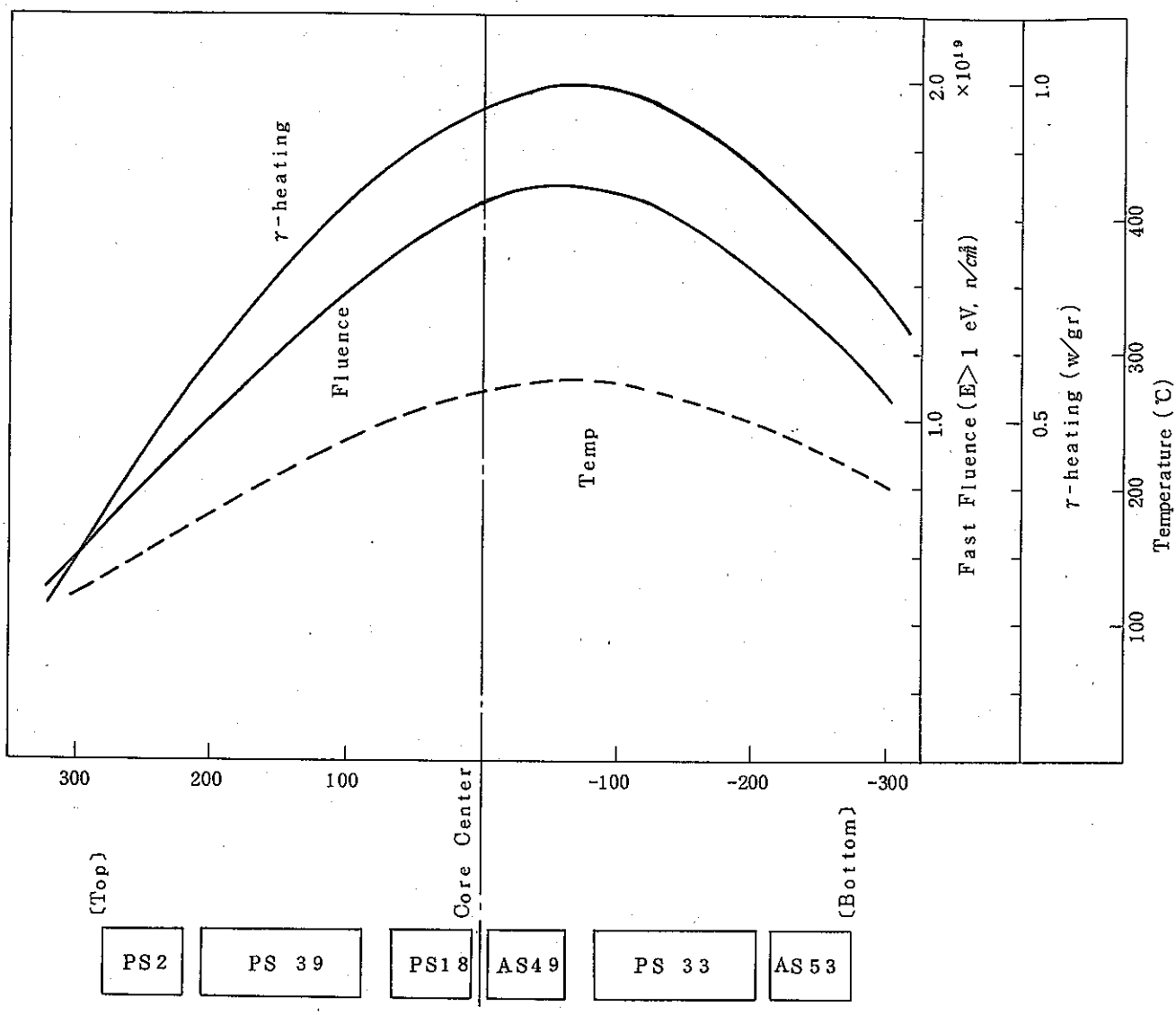

Average Value	PS 2	PS 39	PS 18	AS 49	PS 33	AS 53
Fluence×10^{-19} (E>1MeV)	0.75	1.2	1.6	1.7	1.6	1.3
Temperature (℃)	150	200	260	280	260	220

Fig. 8 Irradiation Condition (Estimated Value)

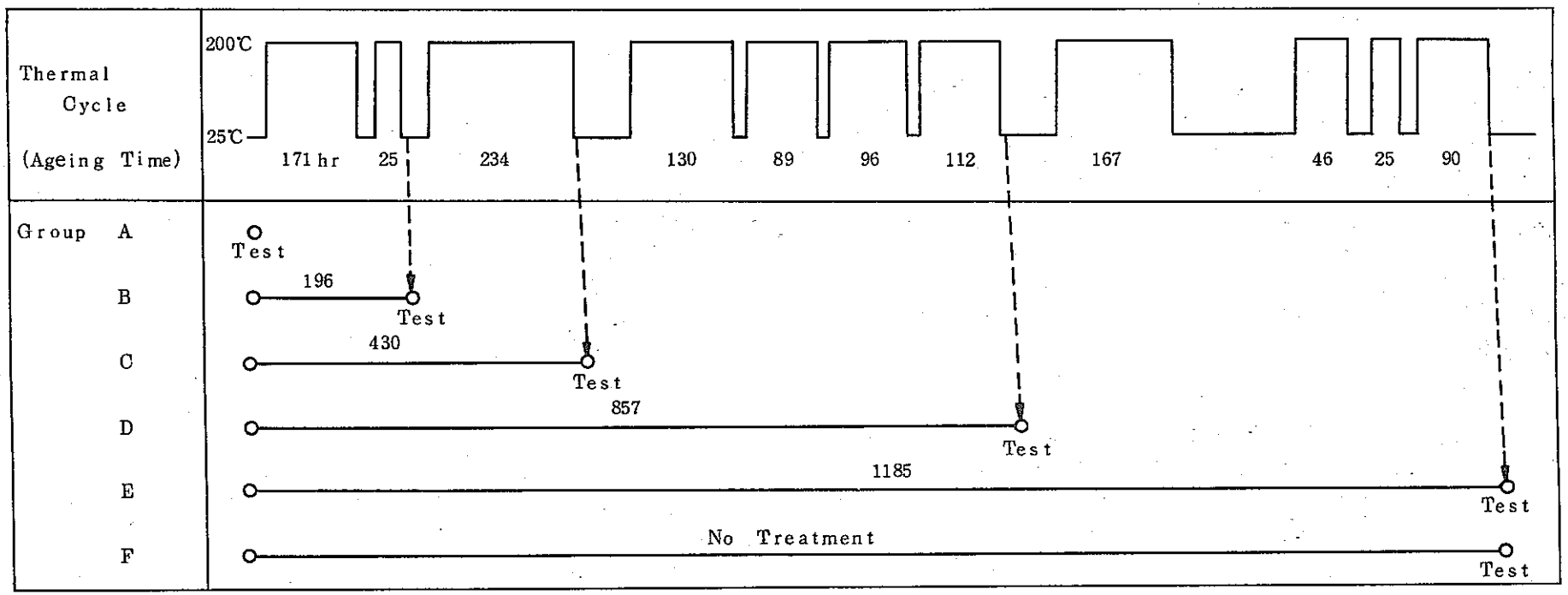

Fig. 9 Thermal Cycle for Serpentine Concrete

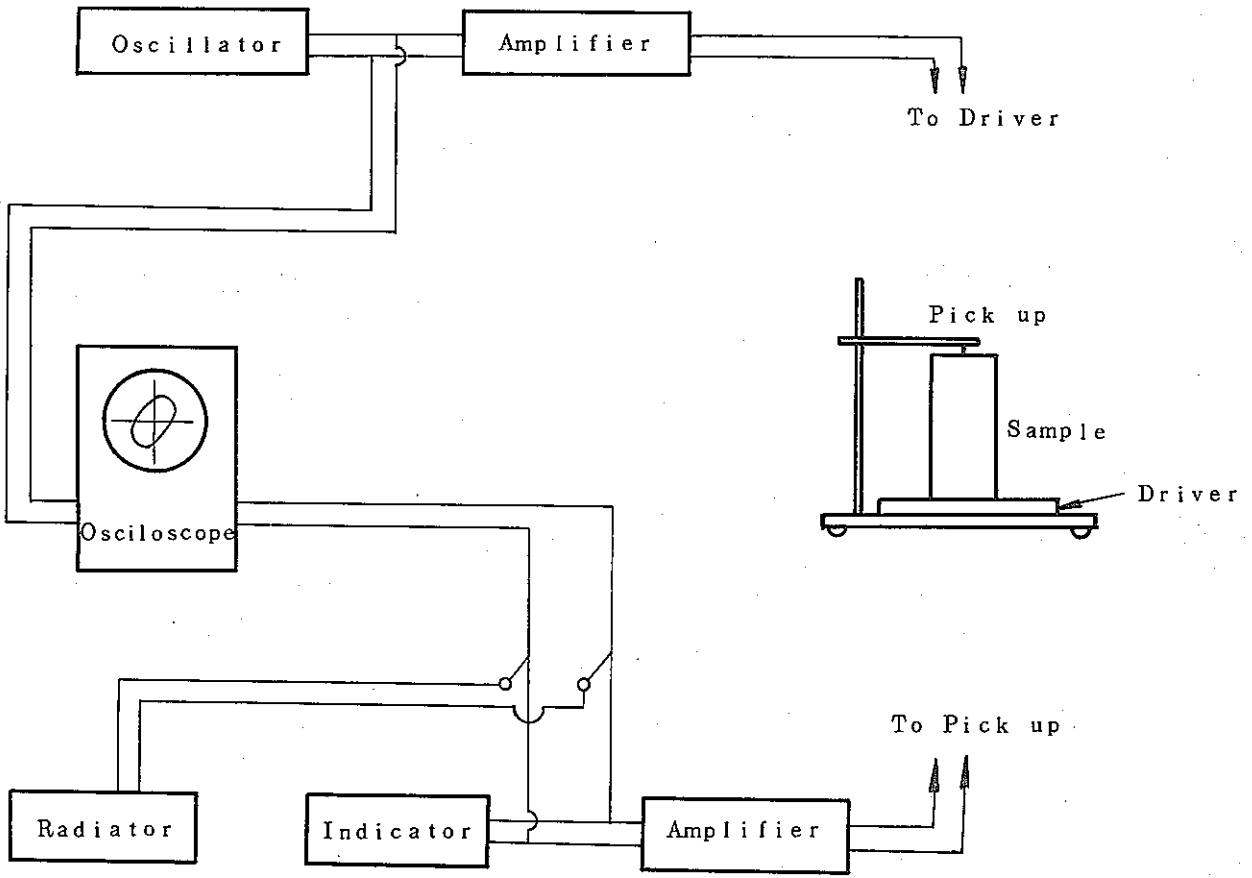

Fig. 10 Block Diagram of Young's Modulus Measurement Apparatus

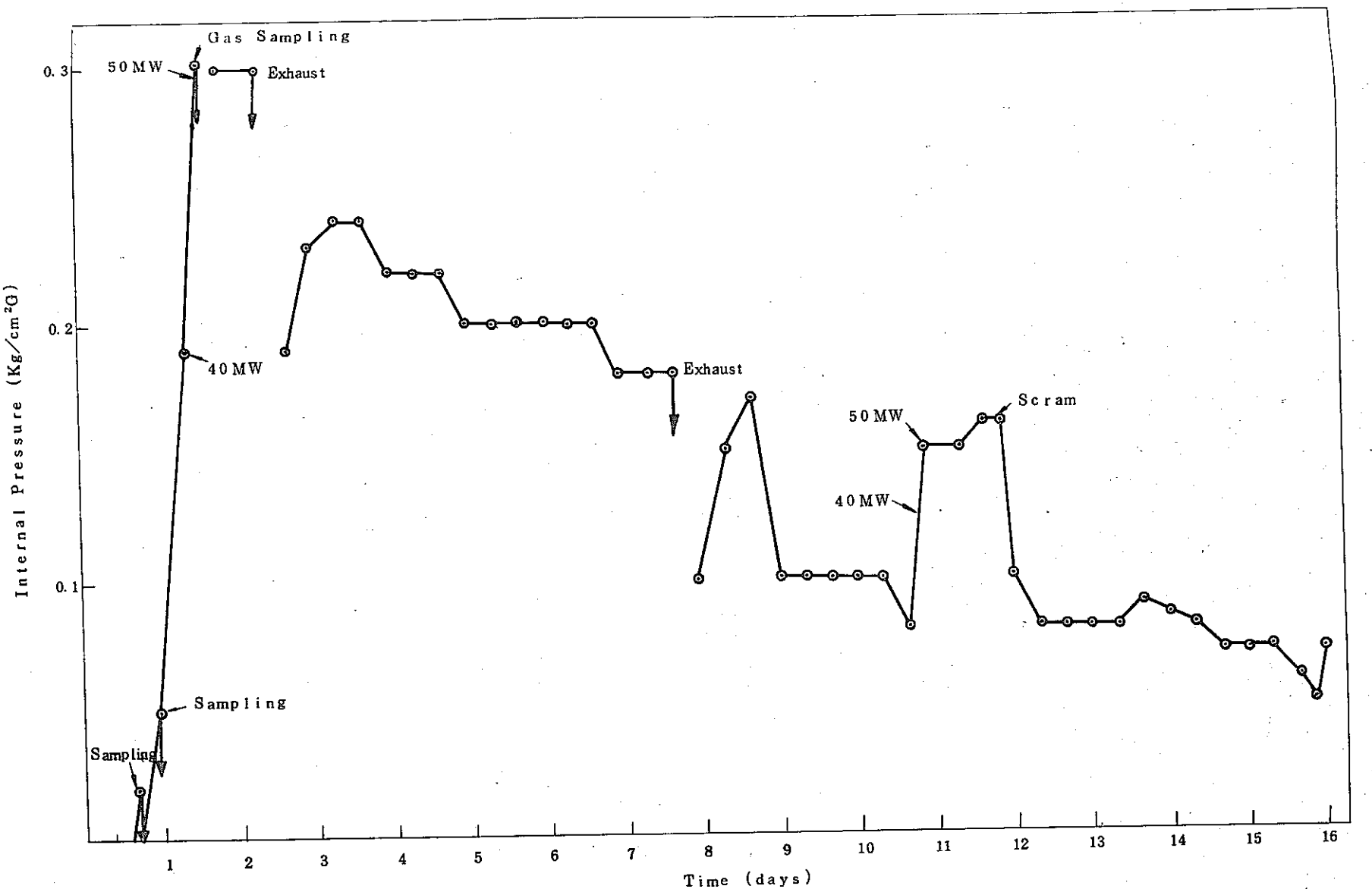

Fig. 11 Internal Pressure of JMTR-SH(I) Capsule

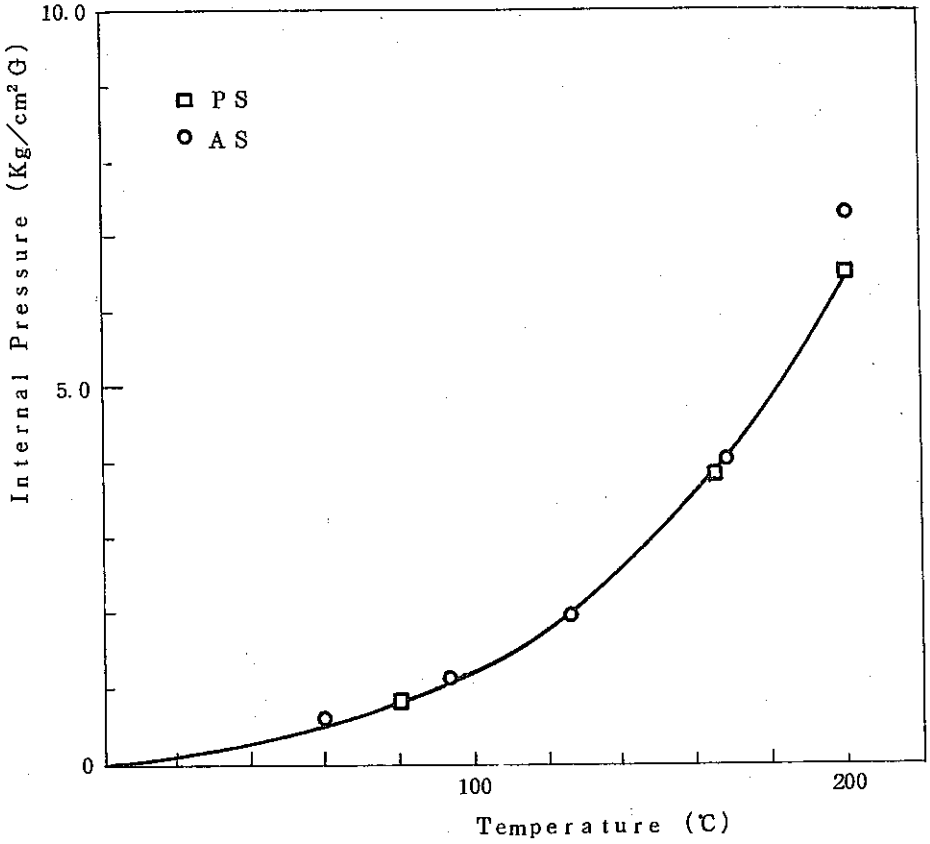

Fig. 12 Internal Pressure of Container

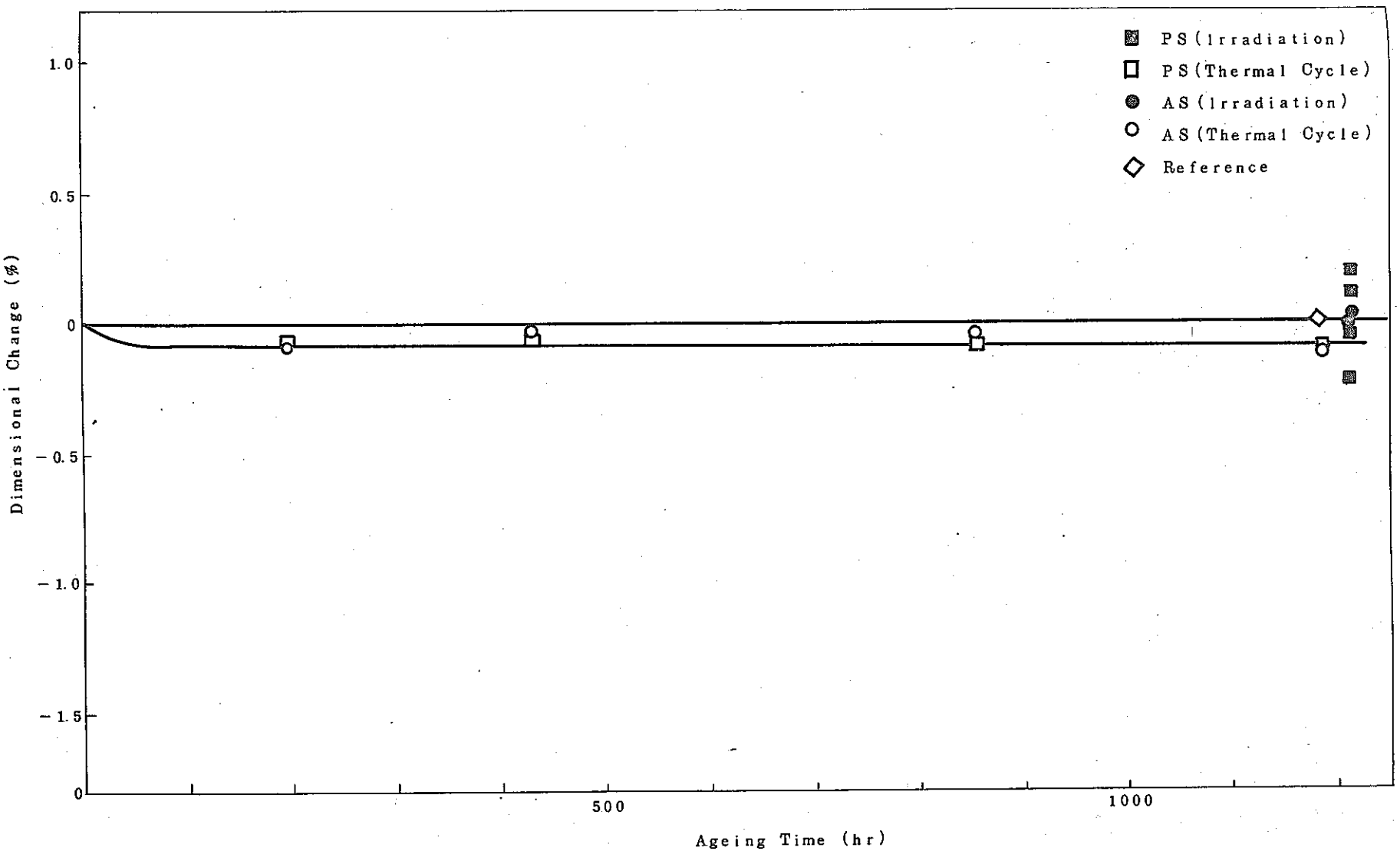

Fig. 13 Dimensional Change of Serpentine Concrete

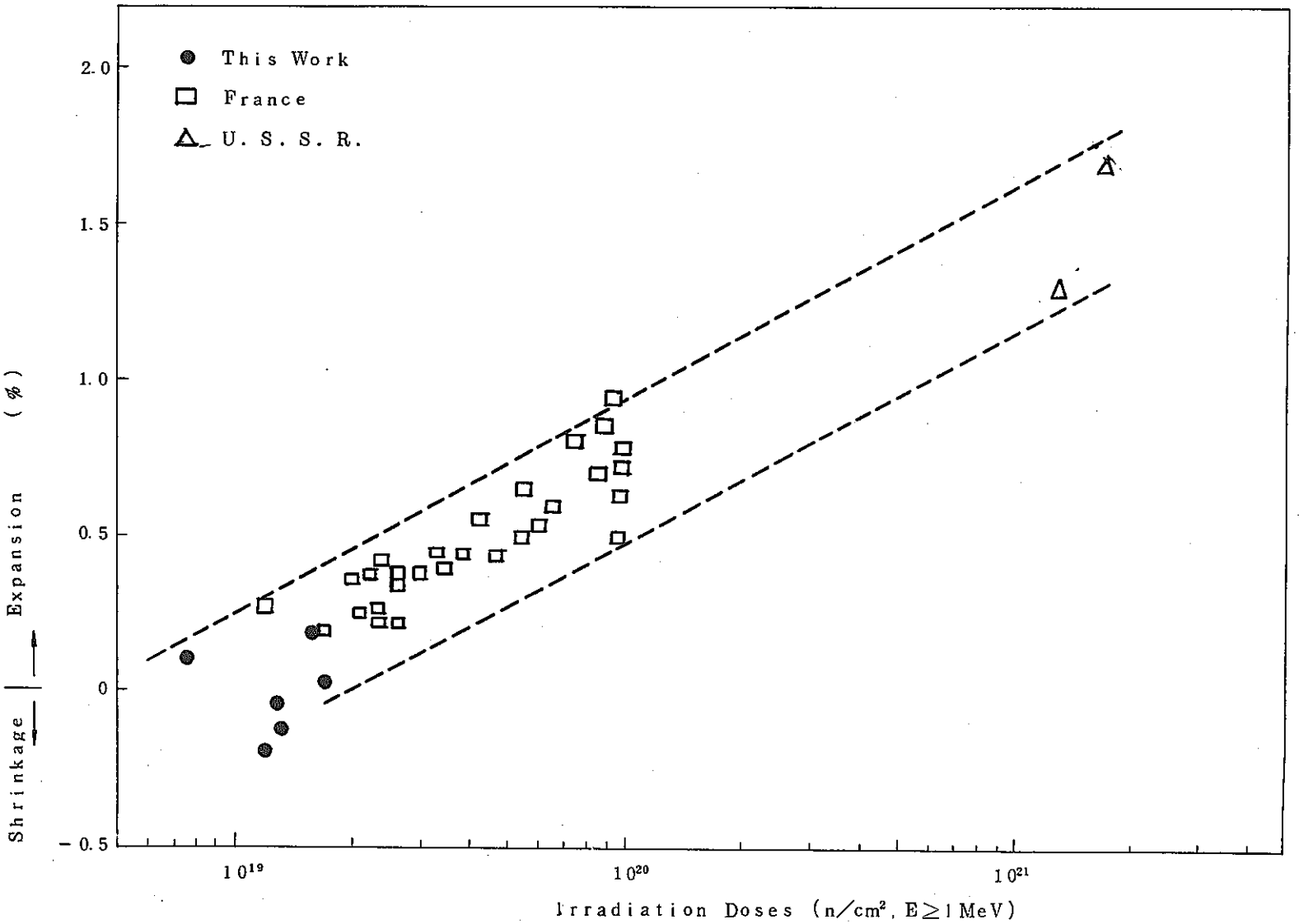

Fig. 14 Neutron Fluence Dependence of Dimensional Change

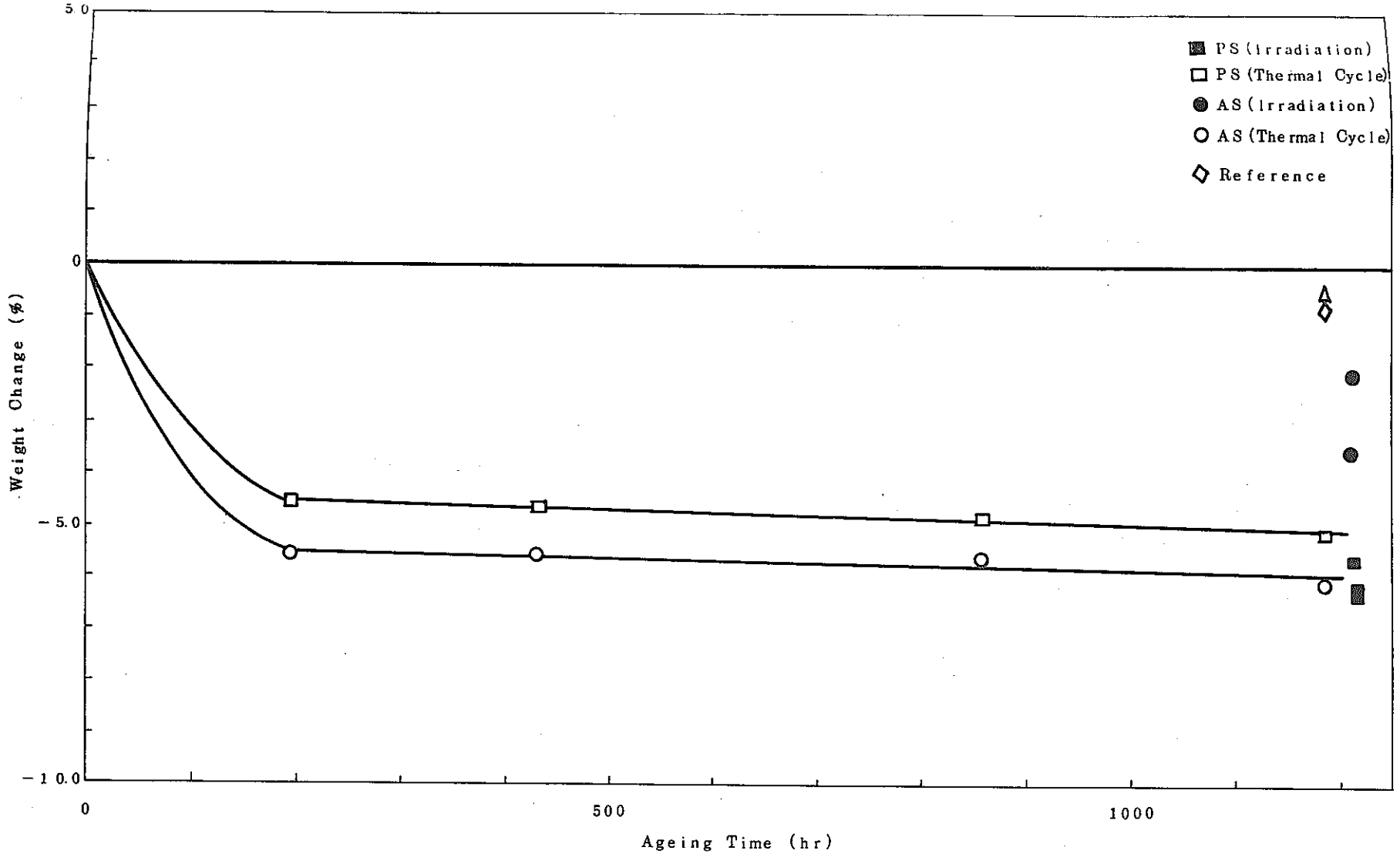

Fig. 15 Weight Change of Serpentine Concrete

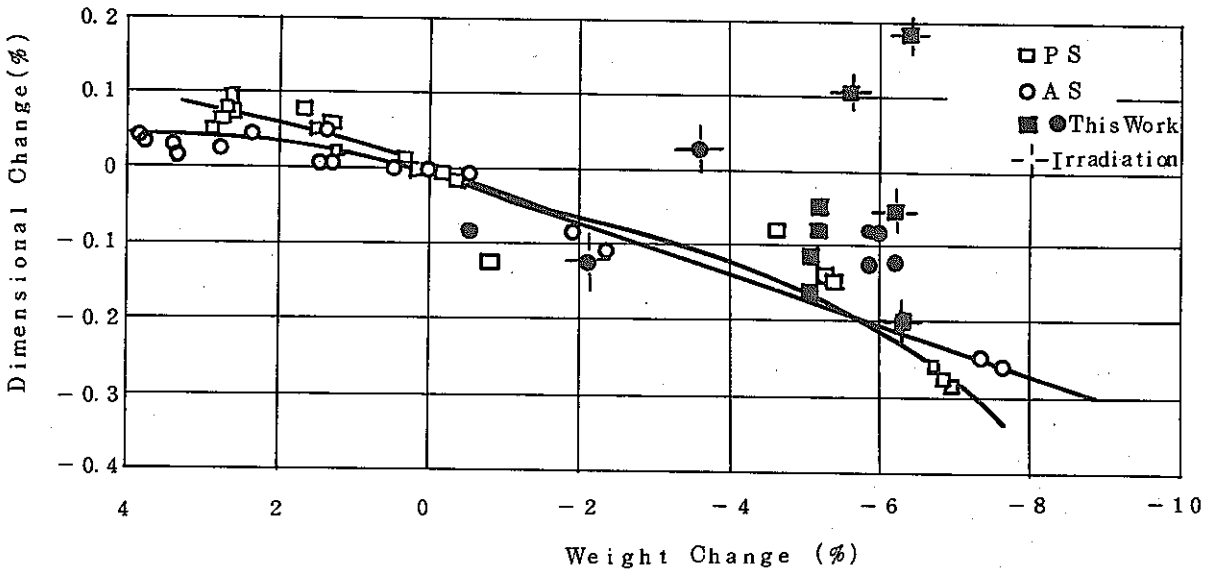

Fig. 16 Relation between Weight Change and Dimensional Change

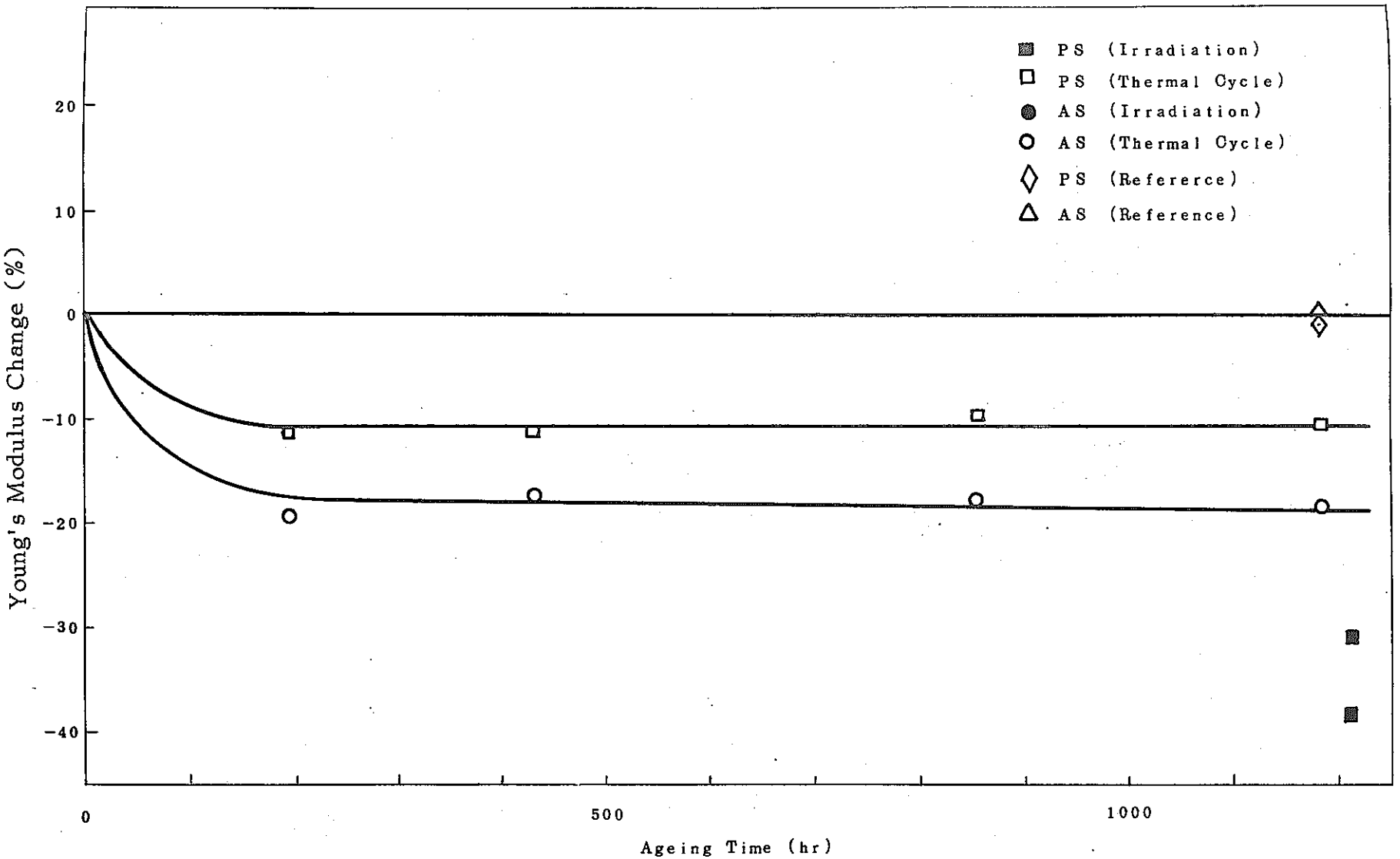

Fig. 17 Young's Modulus Change of Serpentine Concrete

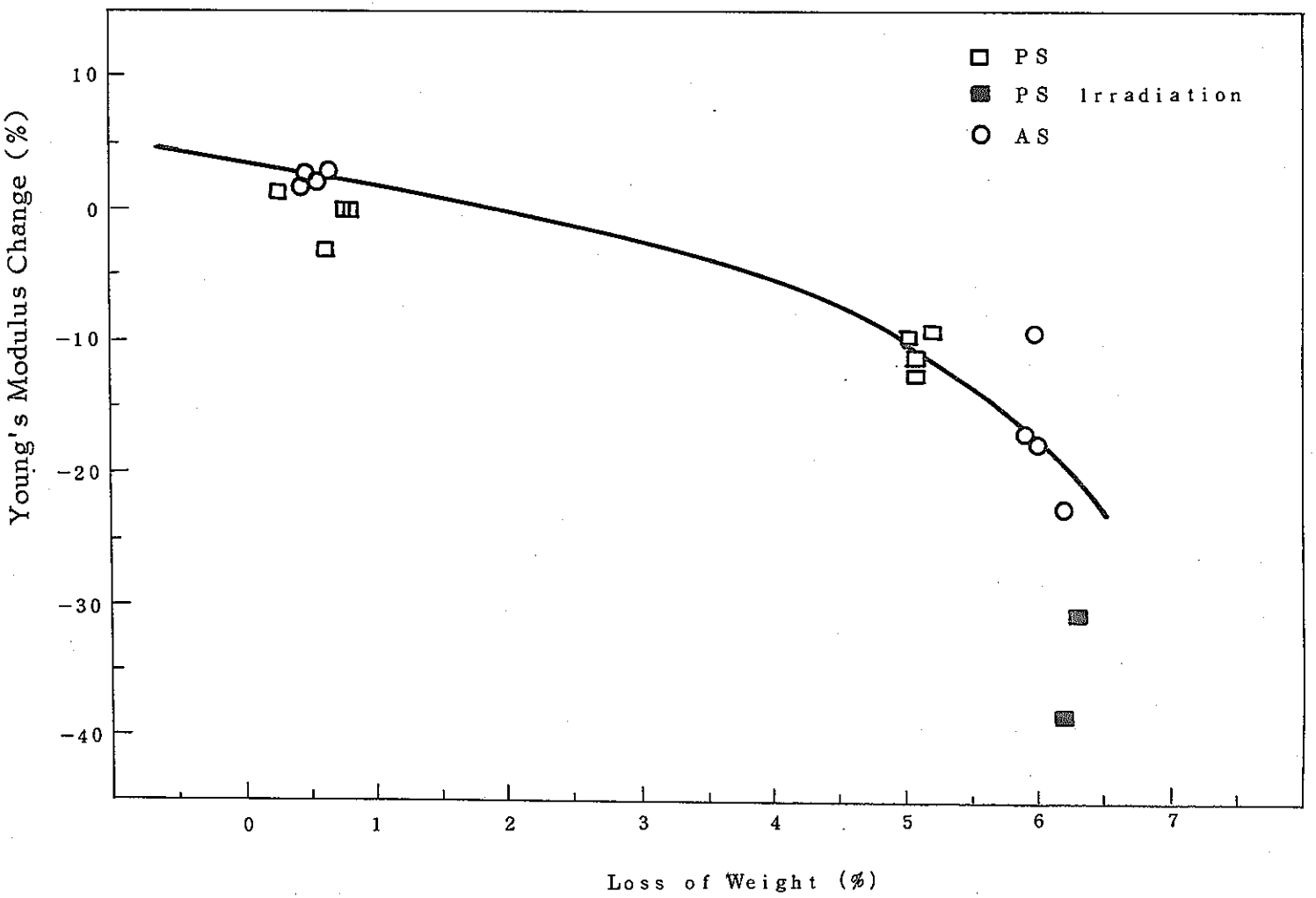

Fig. 18 Relation between Young's Modulus and Weight

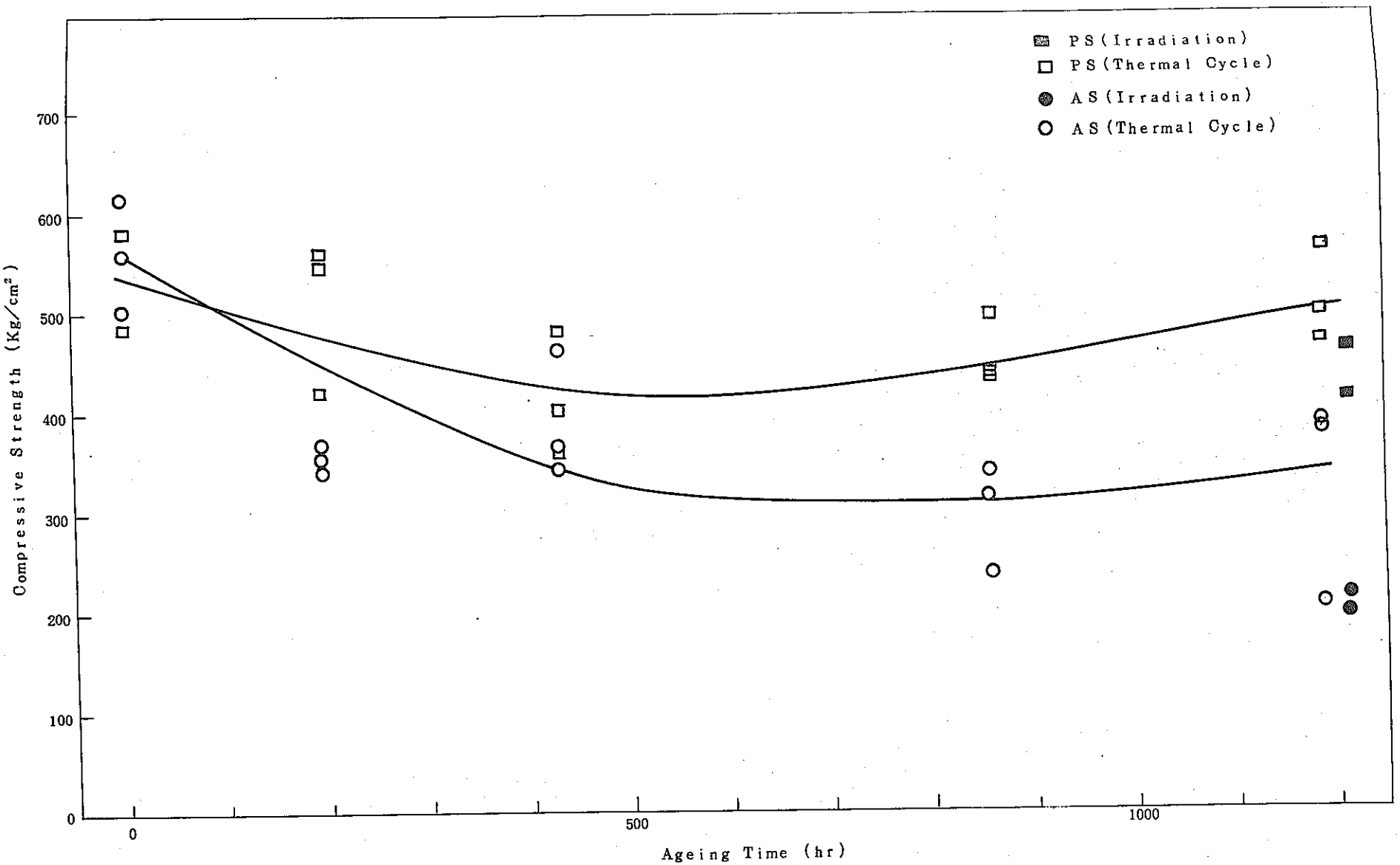

Fig. 19 Compressive Strength of Serpentine Concrete

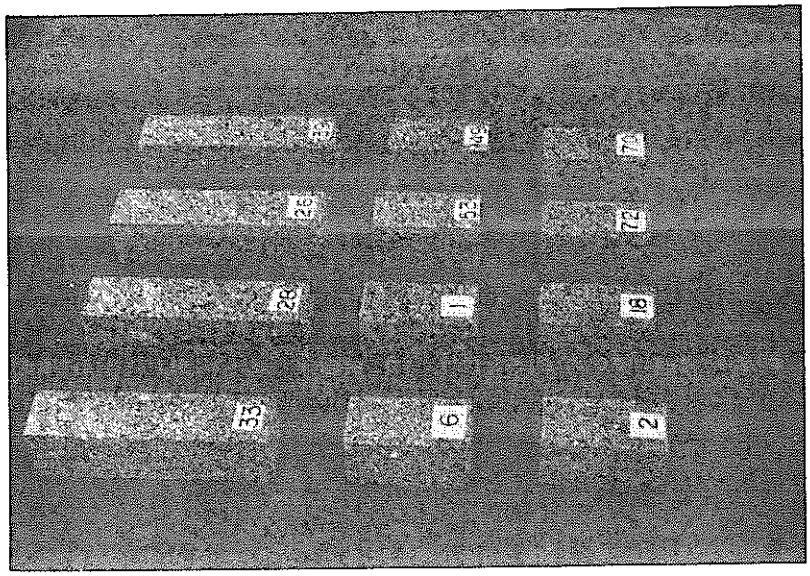

Photo.1 General View of Serpentine Concrete

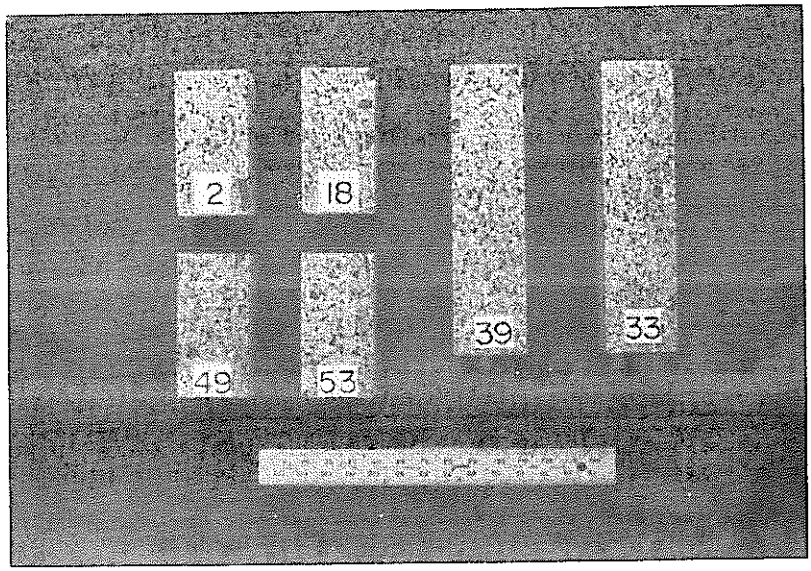

Photo. 2 General View of Irradiation Specimen

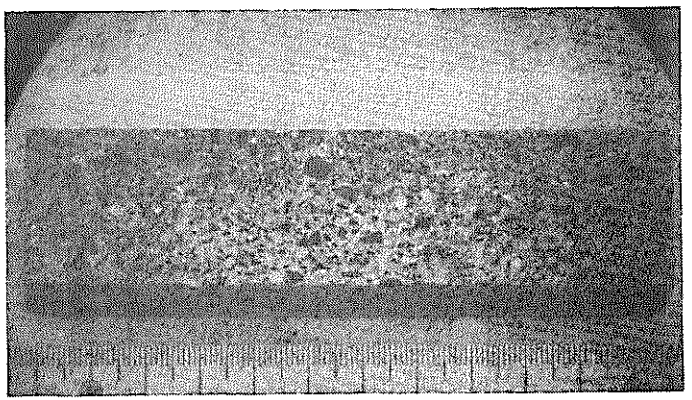

(a) PS−33

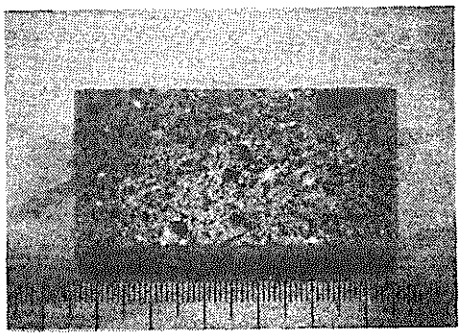

(c) PS−2

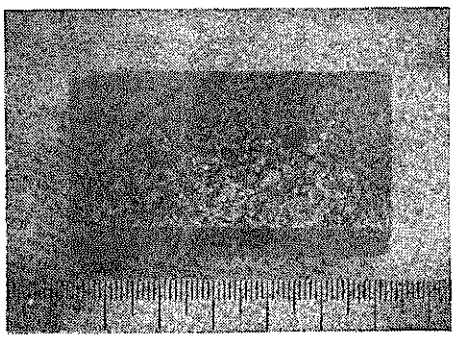

(e) AS−49

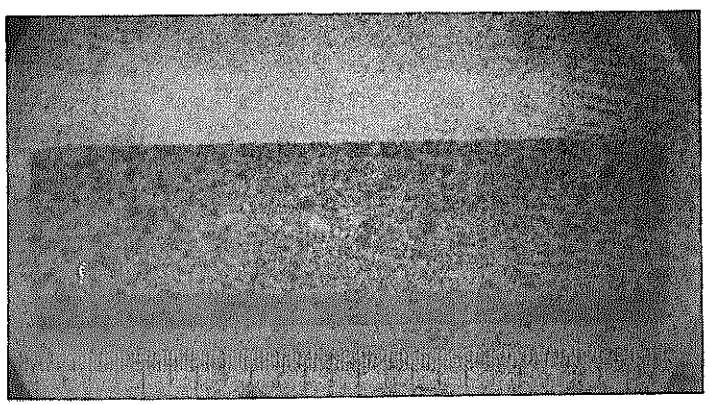

(b) PS−39

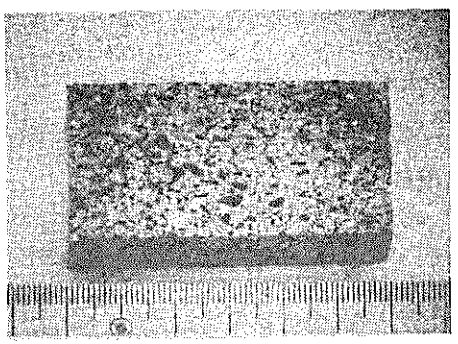

(d) PS−18

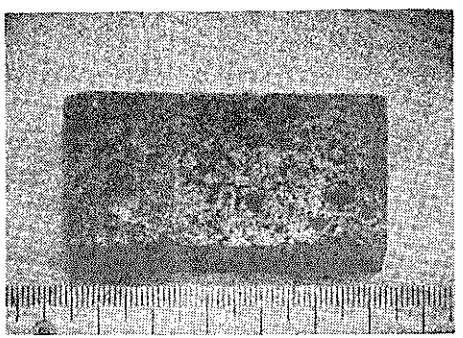

(f) AS−53

Photo.3 General View of Irradiated Serpentine Concrete

(a) Un-irradiation (PS)

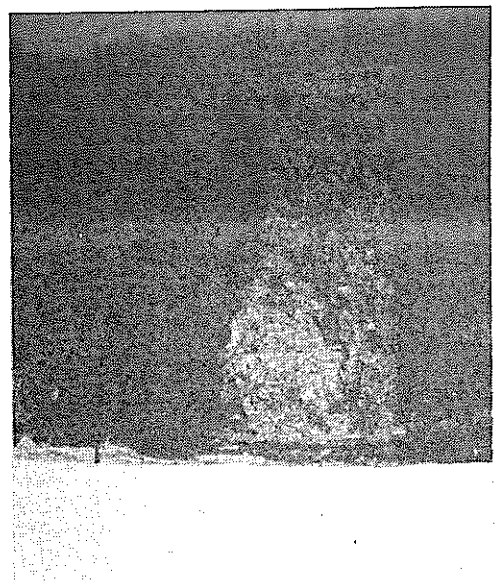

(c) Un-irradiation (AS)

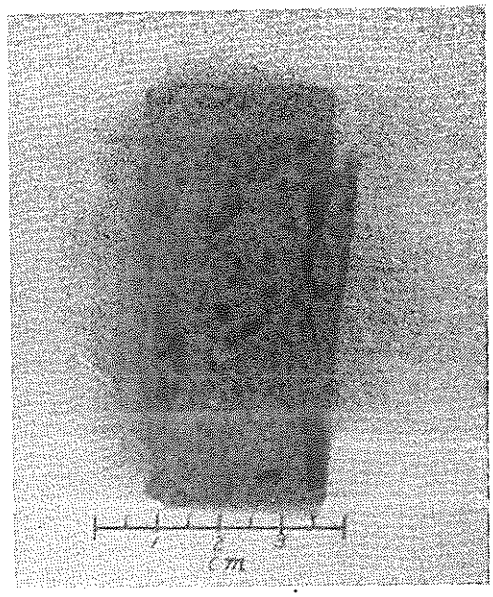

(b) Post-irradiation (PS)

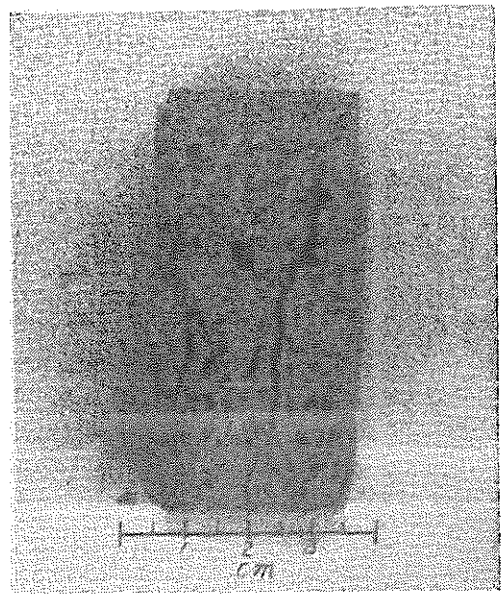

(d) Post-irradiation (AS)

Photo.4 General View of Serpenline Concrete after Compression Test.

APPENDIX

APPENDIX-I

Cement

1.1 Hydration Reaction

In the hydration of ordinary portland cement, its main mineral ingredients of $3CaO \cdot SiO_3$ and $2CaO \cdot SiO_3$ react as follows to form a hydrate of gelled calcium silicate and lime hydroxide. Chemical composition of alumina cement is varied widely compared with that of portland cement. Alumina cement on the regular grade contains 3 to 5 % of SiO_2, 39 to 53 % of Al_2O_3, 1 to 16 % of Fe_2O_3, 36 to 39 % of CaO. Besides, $CaO \cdot 2Al_2O_3$, $12CaO \cdot 7Al_2O$ are contained. According to the chemical composition and the production system, $2CaO \cdot SiO_3$, $2CaO \cdot Al_2O_3 \cdot SiO_2$, etc., are also contained. Mineral components vary widely, however, hydration process is considered as follows.

$$\left.\begin{array}{l} CA \\ CA_2 \\ C_{12}A_7 \\ C_2S \\ C_2AS \end{array}\right\} + H_2O \rightarrow \left\{\begin{array}{l} \text{Hexagonal or quasi-hexagonal} \\ \text{(metastable)} \\ \quad CAH_{10} + C_2AH_8 + C_4AH_{13\sim14} + \\ \quad C_6AH_{30} + C_3S_2H_3 + C_2ASH_8 + Ca(OH)_2 \\ \text{Equiaxial (stable)} \\ \quad C_3AH_6 + AH_3 \end{array}\right.$$

Remarks) C: CaO, A: Al_2O_3, S: SiO_2, H: H_2O

1.2 Impurities

Table 1 shows impurities in the ordinary portland cement. As regards the alumina cement, analysis of impurities has not been made yet, and an example of Lafarge alumina cement is given in Table 2 for

reference. Table 3 shows the quantity of U and Th contained in the cement, and aggregate of serpentine.

1.3 Example of Mixing Proportion for Concrete

Examples of mixing proportion for shielding concrete in Soviet Union and France are shown in Table 5. Such proportion is used for Rapsodie in France.

Table 1. Ordinary portland cement

Chemical composition

Item	Chemical composition (%)								
	(igloss)	(insel)	(SiO_2)	(Al_2O_3)	(Fe_2O_3)	(CaO)	(MgO)	(SO_3)	Total
Analytical value	0.5	0.3	22.3	5.1	2.9	65.0	1.3	1.7	99.1

Besides the above composition, it contains the following chemical substance in quantities shown below.

Item	Micro-chemical composition (PPM)											
	(K_2O)	(Na_2O)	(TiO_2)	(Zn)	(Pb)	(Cu)	(As)	(Cr)	(Mn)	(Co)	(Ni)	(Cd)
Analytical value	5,500	4,500	1,000	1,350	220	208	160	100	100	39	38	41

Table 2. Chemical composition of alumina cement (Lafarge)

Item	Chemical composition (wt %)										
	SiO_2	Al_2O_3	Fe_2O_3	FeO	CaO	MgO	Na_2O	TiO_2	K_2O	CO_2	Total
Analytical value	3.60	39.40	11.00	5.45	38.20	0.10	0.10	1.90	0.03	0.10	99.80

Table 3. U and Th in cement and serpentine (ppm)

Item		U	Th
Serpentine		$10^{-3} \sim 3 \times 10^{-2}$	$< 10^{-3}$
Cement	Limestone	1.3	1.1
	Clay	3.7	12.9

Table 4. Mixing rate of concrete used by

Mixing No.	Materials			Material used in concrete (kg/m3)				Ratio of water to cement (%)	Weight of fresh concrete (t/m3)	Degree of difficulty in placing (sec.)
	Coarse aggregate	Fine aggregate	Pulverlized admixture	Cement	Coarse aggregate	Fine aggregate	Pulverlized admixture			
1	Sandstone	Quartz sand	—	315	1190	678	—	50	2.34	40
2	〃	Fire brick	Fire brick	〃	784	523	305	83	2.18	28
3	Fire brick	〃	〃	288	628	434	288	112	1.96	40
4	Serpentine	Serpentine	Serpentine	253	885	630	253	98	2.27	42

Table 5. Concrete used in Rapsodie (kg/m3)

Alumina cement	Yttrium earth	Corundum 0.2 ~ 2mm	Corundum 2 ~ 5mm	Serpentine 5 ~ 15 mm	Water	Ratio of water to cement
460	150	600	400	1,000	170	0.37

APPENDIX-II

Induced Radioactivity of Serpentine Concrete (calculation)

Details of components of alumina cement, especially impurities, are left unknown and therefore calculation was limited to that of the ordinary portland cement.

(1) Condition

The neutron flux (ϕ) at the irradiation hole I-3 was assumed as follows.

$$\phi th = 5 \times 10^{13}\ n/cm^2 \cdot sec$$

$$\phi f = 5 \times 10^{12}\ n/cm^2 \cdot sec$$

The irradiation time was set to 1213 hours and the cooling time (until measurement of dose rate) was decided to about one year. Composition of ordinary portland cement and that of serpentine are shown in Table 1 in Appendix-I and Table 1 in the report respectively. The mixing rate was as shown in Table 5 in the report.

(2) Calculating Formula

Specific radioactivity (Ci/g) was calculated from the following formula.

Specific radioactivity, $A = N\phi\sigma aS$ [Ci/g]

where,

N : Number of relevant atoms (g^{-1})

ϕ : Neutron flux ($n/cm^2 \cdot sec$)

σa: Absorption cross section (cm^2)

S : $(1 - e^{-\lambda t})$: Saturation coefficient

λ : Disintegration constant of radionuclide (s^{-1})

t : Irradiation time (s)

(3) Results

Results of quantitative calculation of radionuclide formed by thermal neutron are shown in Table 6. Other than those shown in this Table, $^{66}_{Cu}$(0.5mCi), ^{65}Zn(0.6mCi) and ^{69}Zr(0.5mCi) were formed immediately after irradiation. Besides, ^{54}Mn formed by ^{54}Fe(n, p)^{54}Mn reaction is conceivable as a radionuclide. This quantity is about 230 μ Ci immediately after irradiation and about 100 μ Ci after one year.

Accordingly, ^{60}Co, ^{54}Mn and ^{59}Fe are expected to be the γ -ray emitters which may be detectable after one year from an irradiation. These are about 700μCi as ^{60}Co.

Table 6. Induced Radioactivity of Concrete

Nuclide	Radioactive rays and energy(MeV)	Quantity of parent nuclide contained in 1g of concrete (g)	Quantity of saturated formation (mCi)	Half life	Quantity of formation after irradiation for 1213 hours. (mCi)	One year after the irradiation (Ci)
^{24}Na	β^- 4.17 1.389 γ 1.369 2.754	8.7×10^{-3}	21	14.96 hr	21	0
^{27}Mg	β^- 1.75 γ 0.84 1.013	1.6×10^{-2}	14	9.46 m	14	0
^{28}Al	β^- 2.85 γ 1.78	1.9×10^{-2}	140	2.31 m	140	0
^{31}Si	β^- 1.48 γ 1.26	4.6×10^{-3}	14	2.62 h	14	0
^{42}K	β^- 3.52 γ 1.52	4.4×10^{-5}	1.1	12.36 h	1.1	0
^{56}Mn	β^- 2.85 γ 0.847 1.81 2.11	6.1×10^{-4}	120	2.576 h	120	0
^{55}Fe	E.C. Mn X	2.5×10^{-3}	110	2.60 y	4.0	3100
^{59}Fe	β^- 1.57 0.475 γ 1.095 1.29 0.192	1.4×10^{-4}	2.3	45.6 d	1.2	4.6
^{60}Co	β^- 1.48 0.314 γ 1.17 1.33	8.2×10^{-5}	42	5.26 y	0.76	666
^{64}Cu	β^- 0.573 β^+0.656 γ 0.511 1.34	3.8×10^{-5}	2.2	12.8 h	2.2	0
^{76}As	β^- 2.97 γ 0.559	2.5×10^{-5}	1.2	26.4 h	26.4	0

APPENDIX-III

Post-Irradiation Examination at JMTR Hot Laboratory

Table 7 shows the results of irradiation cycle of JMTR-SH(I) capsule. After the irradiation, the capsule was inspected at JMTR Hot Laboratory as a part of post-irradiation examination work before transfered to MMF. The results were as follows.

1. Visual Inspection

The surface of the capsule showed a lustered metallic color peculiar to stainless steel. Discoloring, corrosion, cracks, etc., were not detected and the integrity of the capsule was retained. Photo. 1 shows the external appearance.

2. X-ray Inspection

Photographs were taken by directions of X and Y against the axial direction of the capsule at accelerating voltage of 300 kV. Results are shown in Fig. 1 and Photo. 2.

3. Disassembly of Capsule

After the visual inspection and X-ray inspection were finished, the capsule was disassembled and the specimen was taken out. The capsule cutting was achieved by dry method. An example of disassembled capsule is shown in Photo. 3.

4. Visual Inspection of Specimen

After taking out from the capsule, the specimen was subjected to visual inspection. The result is shown in Photo. 4. As shown in the Photo. 4, the aluminum foil, with which the specimen was wrapped before irradiation, was considerably corroded by heat and moisture, gas, etc. leaked from the serpentine concrete. However, the serpentine concrete itself was observed without difference.

5. Measurement of Weight

Weight was measured after the capsule disassembling and before the visual inspection. The result is shown in Table 8. For the measurement, 2 units Metler balancer Type-He-20 and P-1200 were used. During the measuring time, temperature in the hot cell was 19 °C and humidity was estimated between 60 to 70 %. Weight was also measured at MMF, but no difference between MMF and JMTR Hot Lab. was found.

6. Measurement of Dose Rate

Dose rate of each specimen was measured at distance of 0.3m and 1m. The result is shown in Table 9. Specific radioactivity calculated from these results were 350 to 560 μ Ci/g (as ^{60}Co) in the case of serpentine concrete of ordinary portland concrete of alumina cement. These values are agreeable to reported value (700 μ Ci/g as ^{60}Co) obtained from calculation.

Table 7. Irradiation History Record

No.	
Date	

Capsule No.	71M−84P

Examination title	Effects of irradiation on serpentine concrete
Requested by	Power Reactor and Nuclear Fuel Development Corporation
Examination period	

Capsule type (T/C, F/M) etc.)	Special reglector Mixed gas temperature control
Irradiating hole	I − 3
Irradiati cycle	24 ～ 27

Expected fluence (location, etc.)	Over 10^{19} nvt
Desired irradiation temperature (location, etc.)	In the center of specimen Below 300℃

Number of cycles	Irradiation cycle			Irradiation time		Fluence		Irradiation temperature		Remarks
	Name	Starting date	Date of termination	Classified by cycle	Integrated	Classigied by cycle	Integrated	Average for cycle	Maximum cycle	
1	24	48.11.19	48.12.15	446.4hr	446.4hr	5.8×10^{18}	5.8×10^{18}	℃	℃	Gas sweep
2	25	49. 1.24	49. 2.18	431.0hr	877.4hr	7.2×10^{18}	1.3×10^{19}	℃	℃	Extended for 1 cycle due to trouble occurring in cycle 26
3	26	49. 3.11	49. 3.18	158.4hr	1,035.8hr	2×10^{18}	1.5×10^{19}	℃	℃	
4	27	49. 5.13	49. 5.26	177.0hr	1,212.8hr	2×10^{18}	1.7×10^{19}	℃	℃	Stopped for cycle 26,27 due to trouble of control rod.
5	28	Stopped		hr	hr			℃	℃	PIE schedule
6				hr	hr			℃	℃	1. Cycle date shows power start and power stop.
7				hr	hr			℃	℃	2. Irradiation time is converted to values of 50MW.
8				hr	hr			℃	℃	3. Fluence: Estimated
9				hr	hr			℃	℃	Unit: n/cm² (>1MeV)
10				hr	hr			℃	℃	Location: Peak
										4. Temperature:

Department of Material Testing Reactor,
Japan Atomic Energy Research Institute

Table 8. Weight of specimen after Irradiation

Specimen No.	Weight (g)		
	1	2	Average
PS－ 2	109.970	109.970	109.971
PS－18	109.690	109.699	109.699
PS－49	111.368	111.369	111.369
PS－53	108.183	108.185	108.184
PS－39	215.06	215.07	215.07
PS－33	214.85	214.85	214.85

Measuring conditions

Measuring instrument used	Model Radcon 1555, Victrin Corp.				
Probe type	1HA	Energy calibration coefficient		Cs-137 1.04	Co-60 1.00
Accuracy of measuring instrument	within ±5%	Atmospheric pressure (mmHg)		Calibration coefficient	Within 2%
Energy range	400KeV ~ 1300KeV	Temperature		— 〃 —	

Note

△B.G 5.5 mR/m

B.G included in measured values.

Table 9. Measurement of Total Radioactivity

Specimen №	Measuring distance	Rate. Integrated	Measuring range	Dose rate, dose	Time (min)	Probe amplifier
№ AS-53	0.3	rate	30mR/m	20.2 mR/m		(×1)
	1.0	〃	10mR/m	7.9 mR/m		〃
PS-2	0.3	rate	30mR/m	15.5 mR/m		(×1)
	1.0	〃	10mR/m	7.55mR/m		〃
PS-18	0.3	rate	30mR/m	21.4 mR/m		(×1)
	1.0	〃	10mR/m	8.07mR/m		〃
AS-49	0.3	rate	30mR/m	22.7 mR/m		(×1)
	1.0	〃	10mR/m	8.2 mR/m		〃
PS-33	0.3	rate	100mR/m	37.0 mR/m		(×1)
	1.0	〃	30mR/m	9.58mR/m		〃
PS-39	0.3	rate	100mR/m	31.5 mR/m		(×1)
	1.0	〃	30mR/m	1.1 mR/m		〃

JMTRH.L D-S № 3

Photographing direction, classification of observation

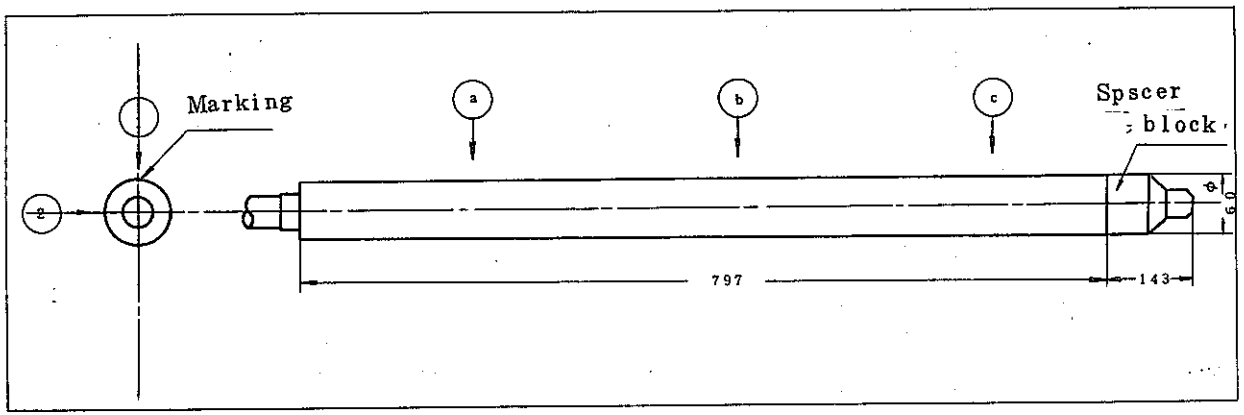

X-ray inspecting conditions

1. Acc. voltage		300 KV
2. Tude current	L S	3.5 mA
3. Exposure time		30 min
4. Film		R
5. Intensifying screen		Pb 0.03mm
6. F.S.D.		1800 mm
7. S.F.D.		360 mm

Film No.	Photographing direction	Photographing position	Observation
75X-167	①	ⓐ	No abnormality observed
75X-165	①	ⓑ	〃
75X-161	①	ⓒ	〃
75X-164	②	ⓐ	〃
75X-166	②	ⓑ	〃
75X-162	②	ⓒ	〃

Notes

1) Magnification of photo: 1.26 approximately
2) Photographing was impossible at the regular position due to the size of the capsule, 60mm in dia., 900mm in length. Consequently, magnification became higher and photo. lost sharpness.

Japan Atomic Energy Research Institute

JMTR·H·L D-S No. 4

Fig. 1 X-ray Test

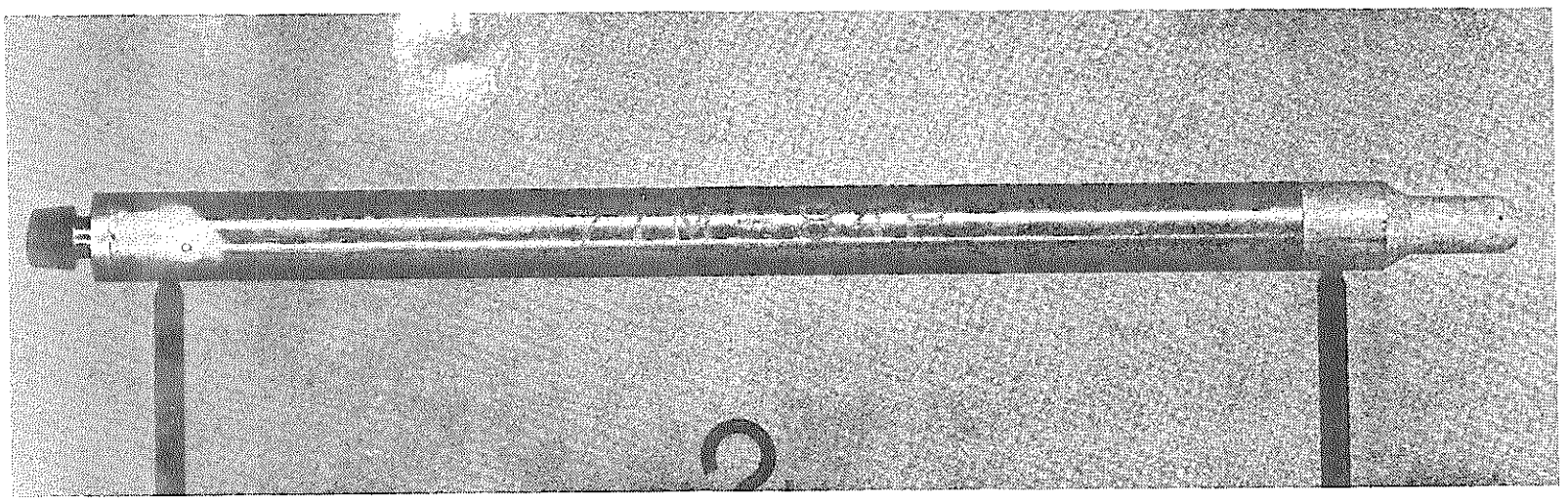

Photo. 1 General View of Capsule

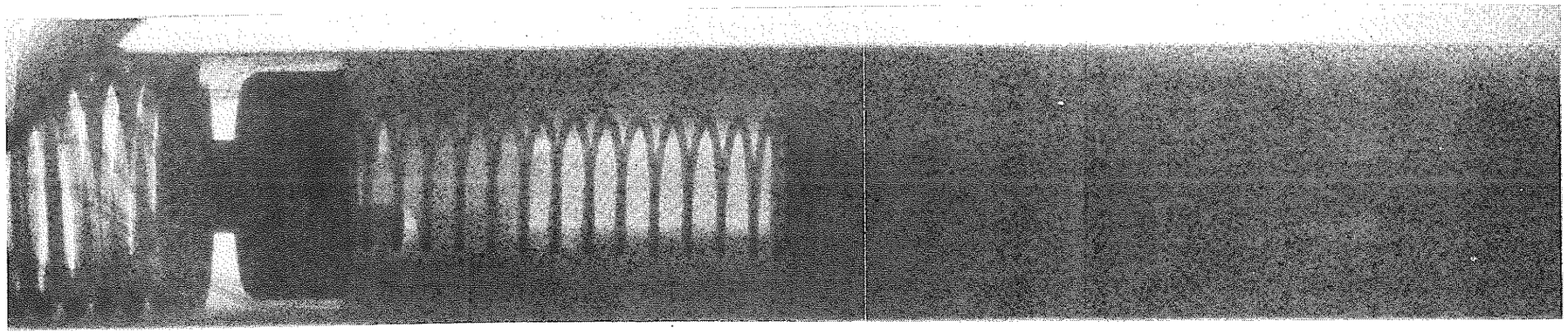

(a)　75X－167

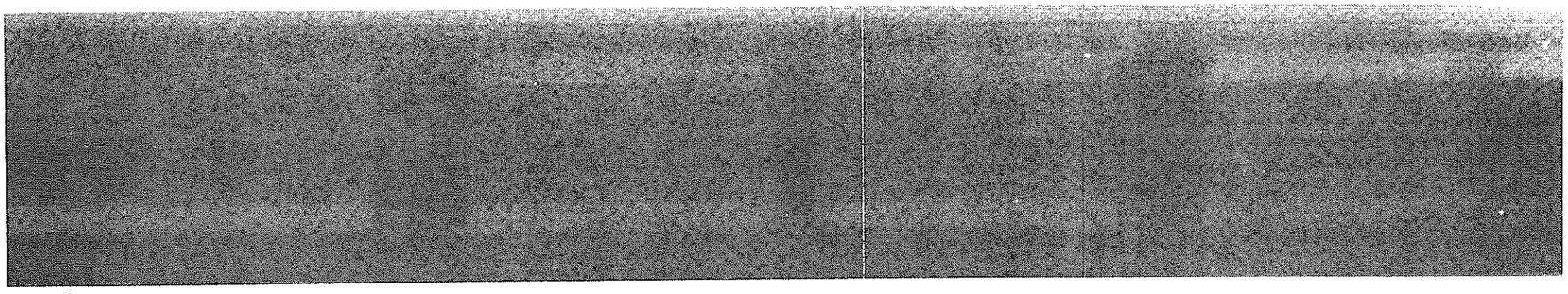

(b)　75X－165

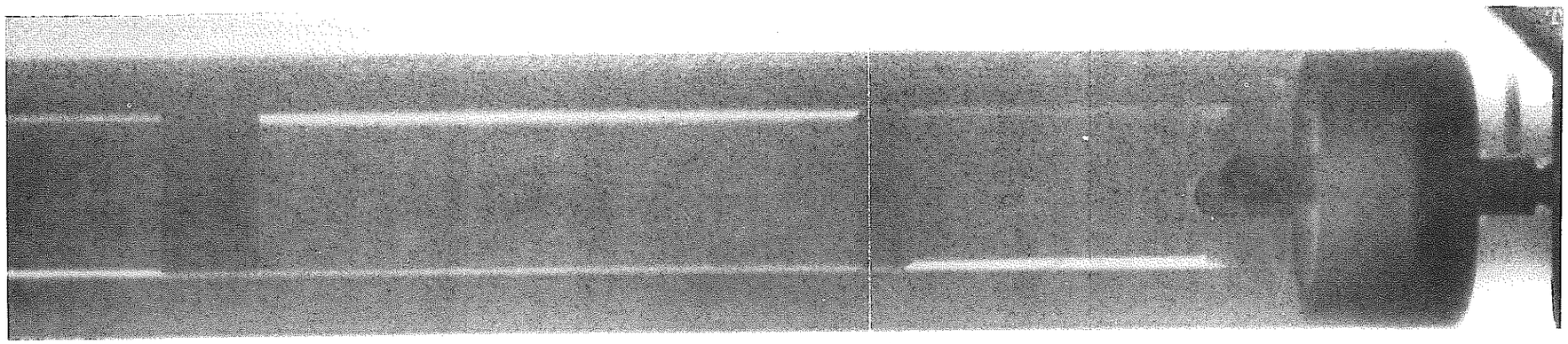

(c)　75X－161

Photo. 2　X-Ray Radiography (1)

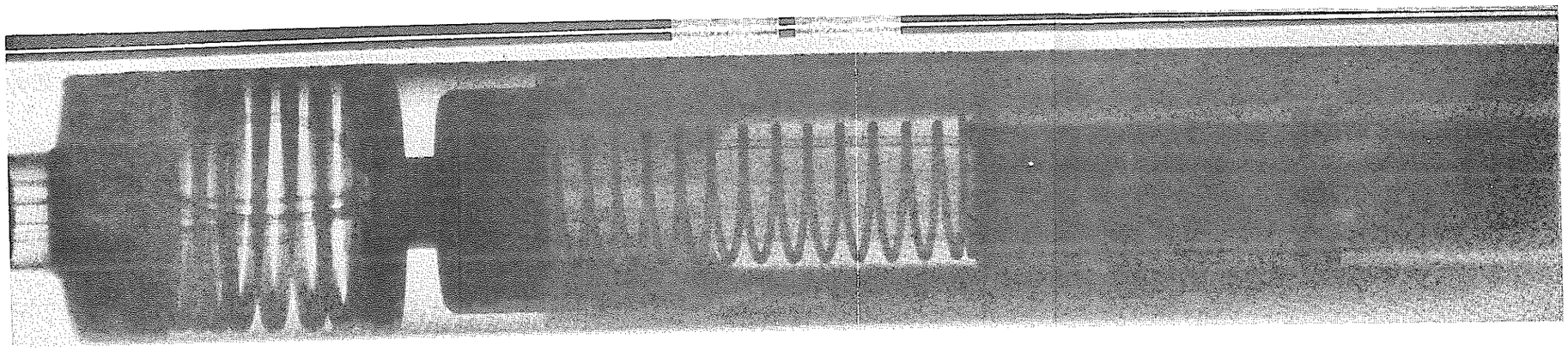

(d) 75X—164

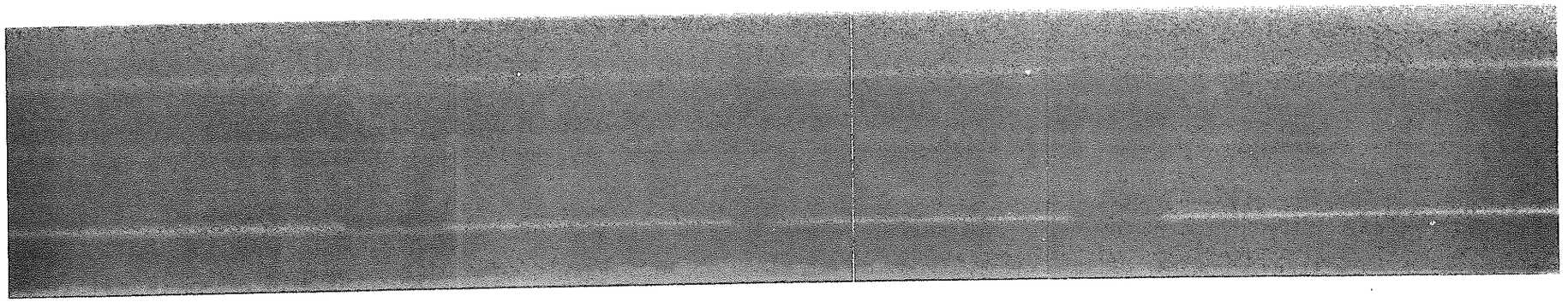

(e) 75X—166

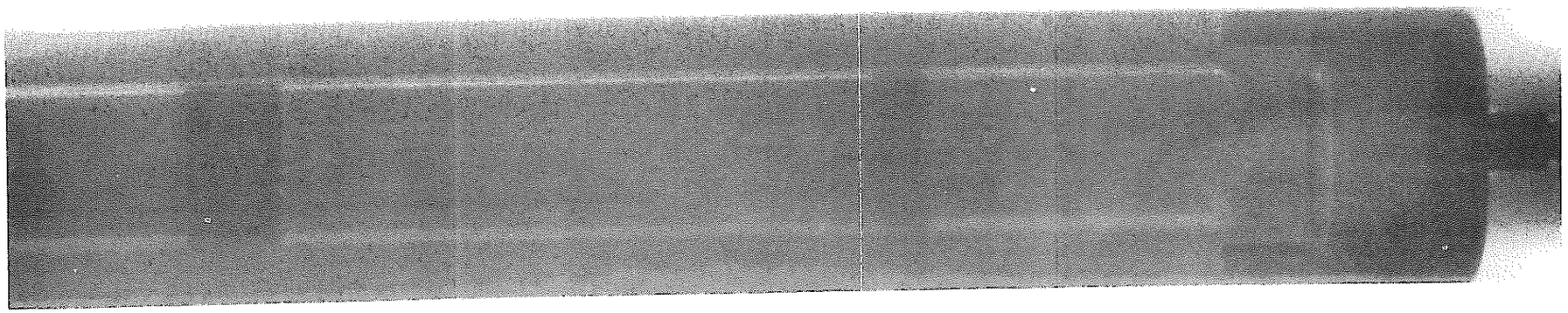

(f) 75X—162

Photo. 2 X-Ray Radiography (2)

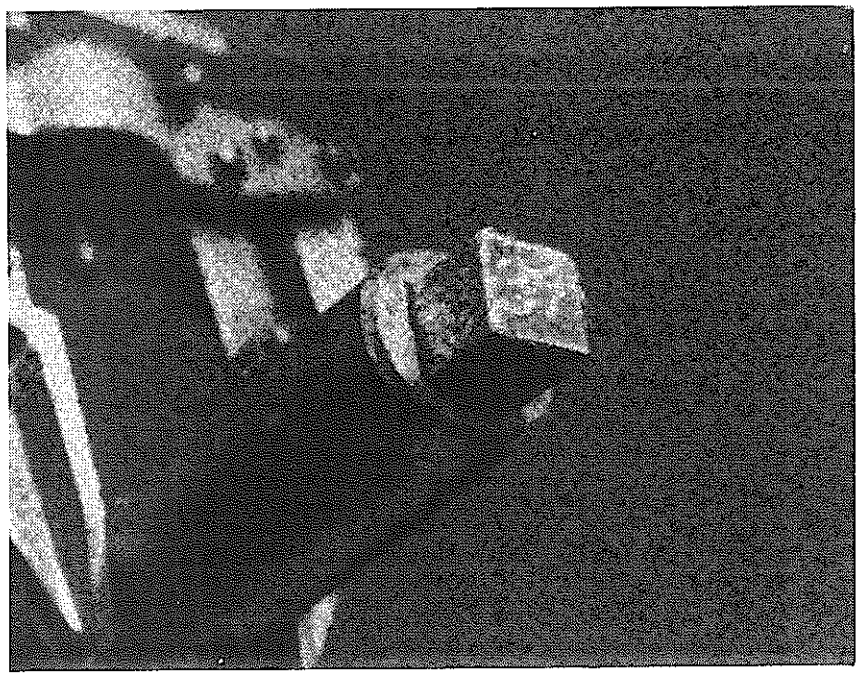

Photo. 3 Capsule and Irradiated Concrete

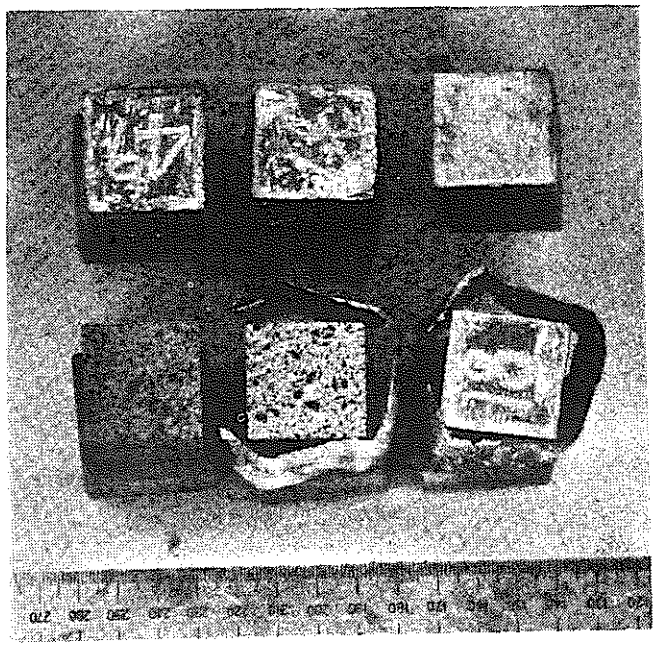

(a)

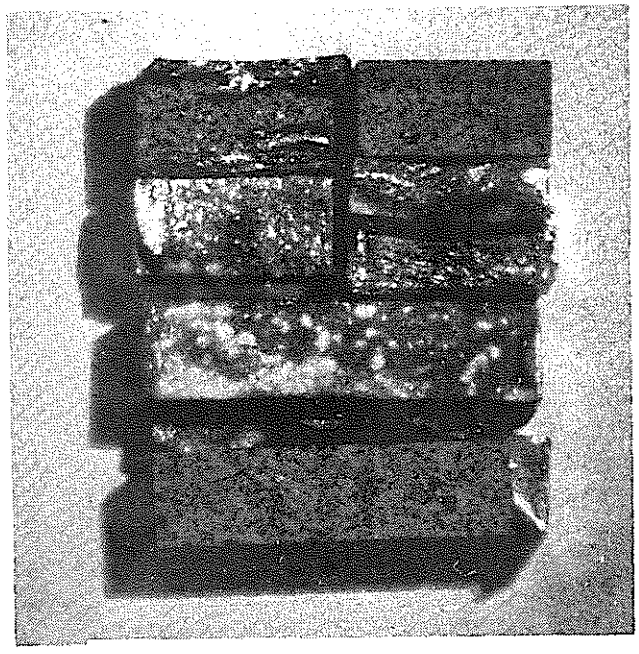

(b)

Photo. 4 General View of Serpentine Concrete

APPENDIX-IV

Thermal Calculation of Capsule

1. Assumptions Used in Calculation

1) Temperature of cooling water is neglected, for the maximum temperature of the specimen (300 °C) is sufficiently low. Accordingly, calculation is made of a specimen alone neglecting the temperature distribution in the cooling water.

2) The heat transfer rate between the cooling water and the other tube is set to a constant value of 2.32 $W/cm^2/^{\circ}C$.

3) Thermal expansion of the specimen and the material of the capsule are taken into account. Heat radiation is neglected because of little effect at low temperature.

4) The square shape of the specimen and the inside of the thermal medium is converted into the equivalent circle and calculation is made using the model of multiple-cyclinder of endless length.

2. Calculating Formula

1) Temperatures difference between inner and outer diameters.

$$\Delta T = \frac{q'}{2\pi k} \ln \frac{r_o}{r_i} + \frac{e}{k} \left\{ \frac{1}{4} (r_o^2 - r_i^2) - \frac{1}{2} r_i^2 \ln \frac{r_o}{r_i} \right\}$$

where,

q' : Total generation of heat in ri (w/cm)

ro : Outer radius (cm)

ri : Inner radius (cm)

e : Generation of heat in $ri \leqq r \leqq ro$ (w/cm^3)

k : Thermal conductivity of substance in $ri \leqq r \leqq ro$ ($w/cm/^{\circ}C$)

2) Temperature difference in the specimen

$$\Delta T = \frac{e}{4k} r_o^2 = \frac{q}{4\pi k}$$

3) Temperature difference between gap

$$\Delta T = \frac{q'}{2\pi k} \ln \frac{(r_i + \Delta r)}{r_i}$$

where,

q' : Total generation of heat in ri (w/cm)

ri : Gap inner radius (cm)

Δr : Gap (cm; one side)

k : Thermal conductivity of gas between gaps (w/cm/°C)

3. Physical values used in calculation (density, thermal conductivity, coefficient of thermal expansion)

1) Density (g/cm^3)

SUS27 : 7.9 (JAERI 2704)

Aluminium: 2.7 (Aluminium Vol. 1 K.R. von Horn)

Specimen: 2.26

2) Thermal conductivity (w/cm/°C)

SUS27 : 0.163 (100°C) 0.178 (200°C) 0.190 (300°C)

Aluminium: $0.20790 + 0.52459 \times 10^{-3}t - 0.74189 \times 10^{-7}t^2$

Specimen: 0.009886 (= 0.85 Kcal/m/h/°C)

3) Coefficient of thermal expansion

SUS27 : 17.3×10^{-6} (10 ~ 100 °C)

Aluminium: $Lt = Lo \{ 1 + (22.34t + 0.0098t) \times 10^{-6} \}$

Specimen: 6.3×10^{-6}

4. Calculating Model

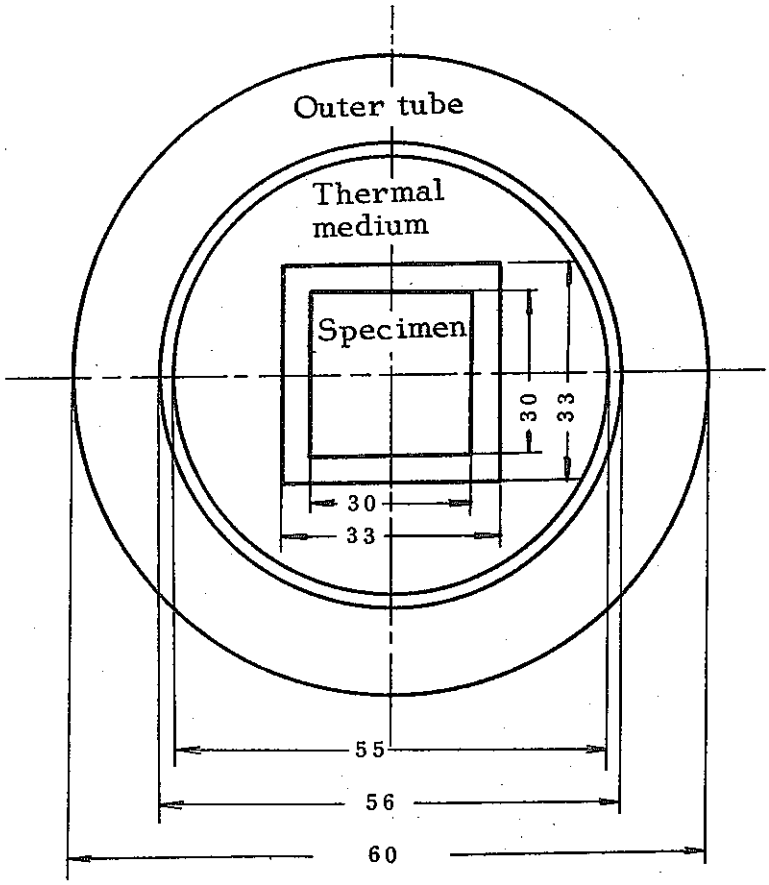

Radius of equivalent circle of specimen:

16.925 mm

Inner radius of medium:

18.426 mm

Outer radius of medium:

27.5 mm

Inner radius of outer tube:

28 mm

Outer radius of outer tube:

30 mm

Fig. 2 Calculating Model

The actually used model is shown above. For calculation with an endless multiple-cylinder, the concrete specimen was converted into equivalent circle.

5. Results of Calculation

Fig. 3 shows the results of temperature calculation at several points using γ -heating value as a parameter.

6. Thermal Calculation at the Japan Atomic Energy Research Institute

Figs. 4 and 5 show the results of calculation by GENGTC.

7. γ-Heating Coefficient

Relative value of γ-heating coefficient in vertical direction of JMTR is shown in Fig. 6 and its relation with reactor power shown in Fig. 7.

8. Irradiation Temperature

The indicated value (by thermocouple) of temperature during irradiation is shown in Fig. 8.

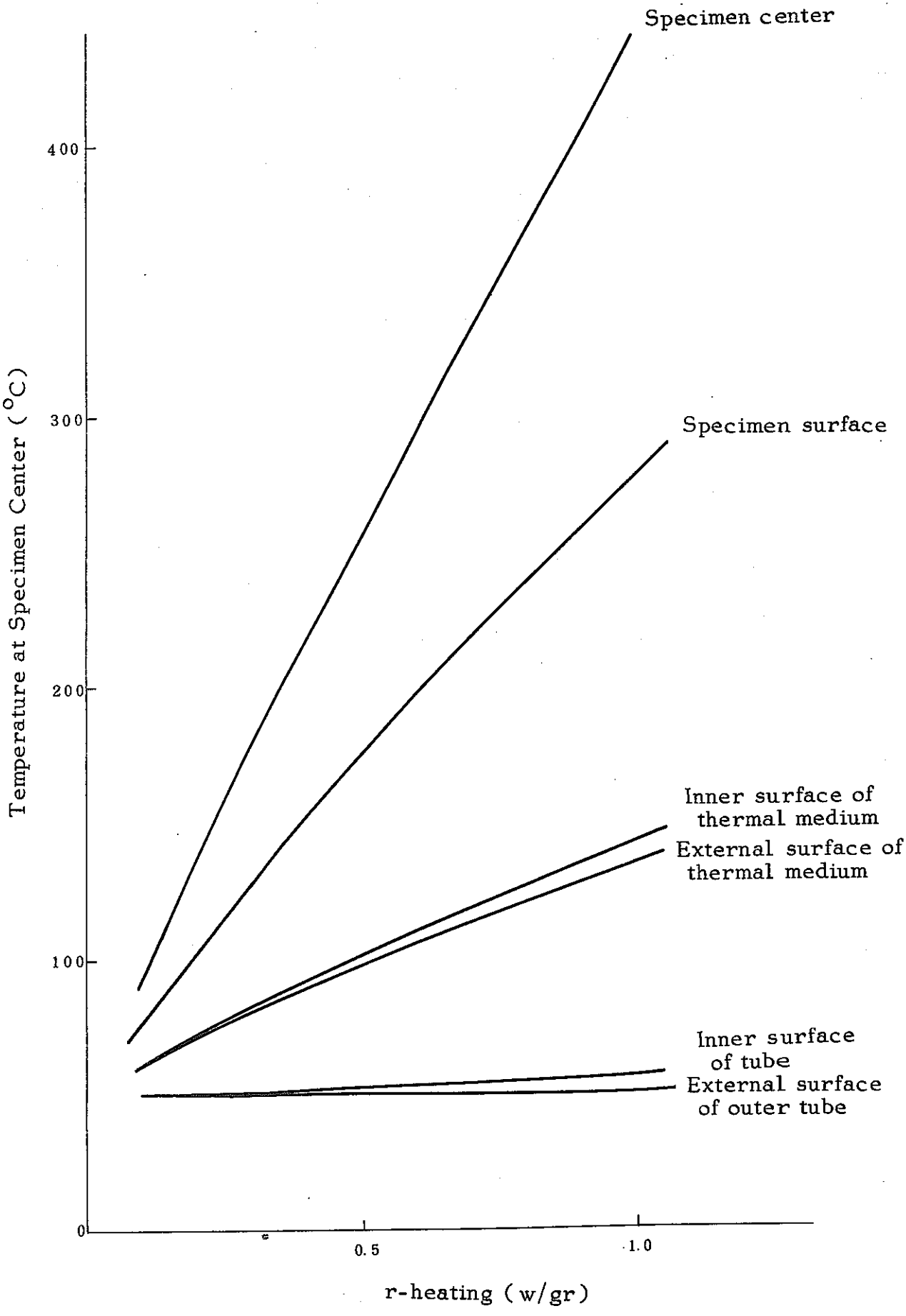

Fig. 2 Relation between r-Heating and Temperature at Specimen Center

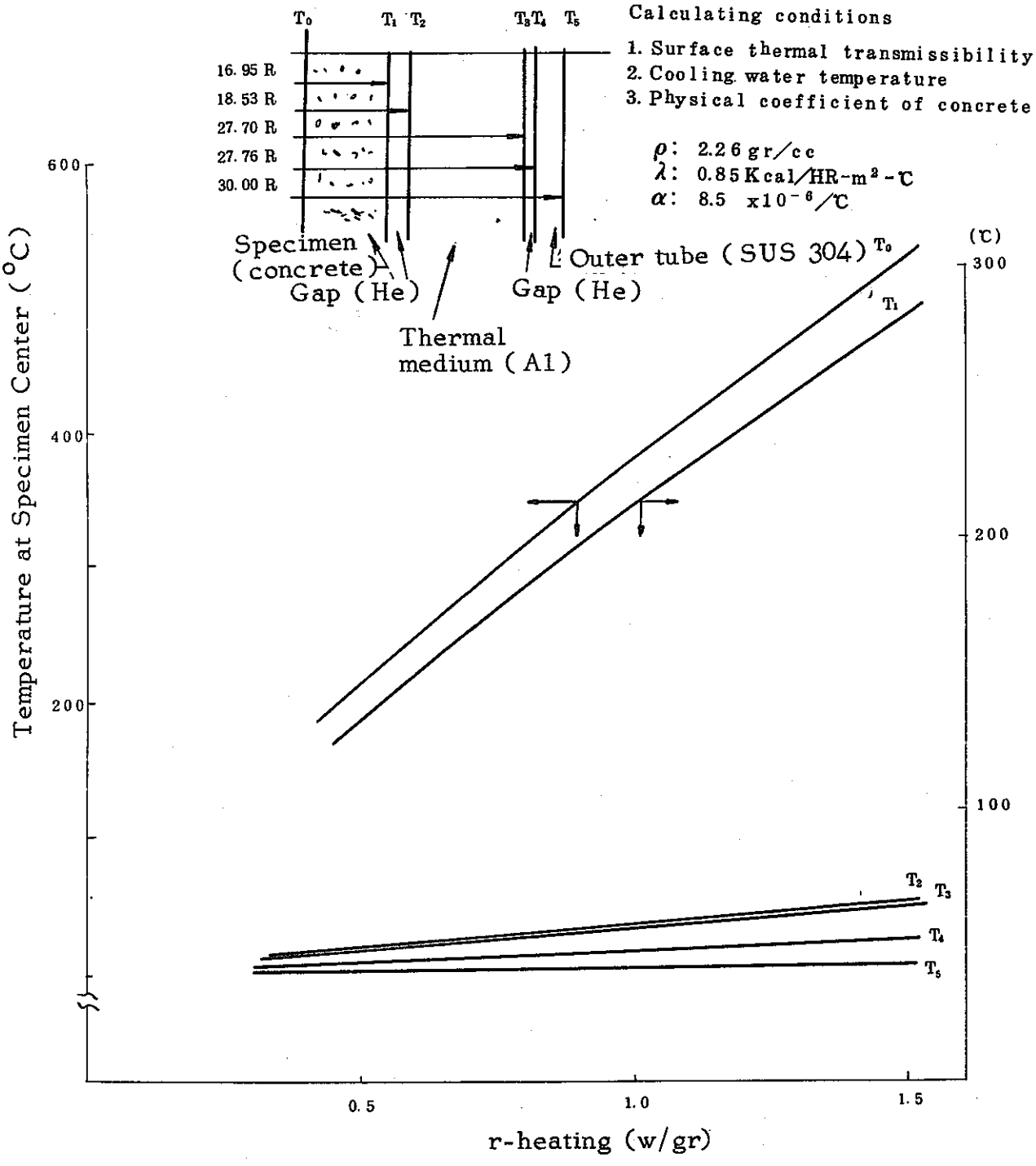

Fig. 4 Temperature Distribution in Capsule for JMTR-SH(I)
(Position of T/C #5)

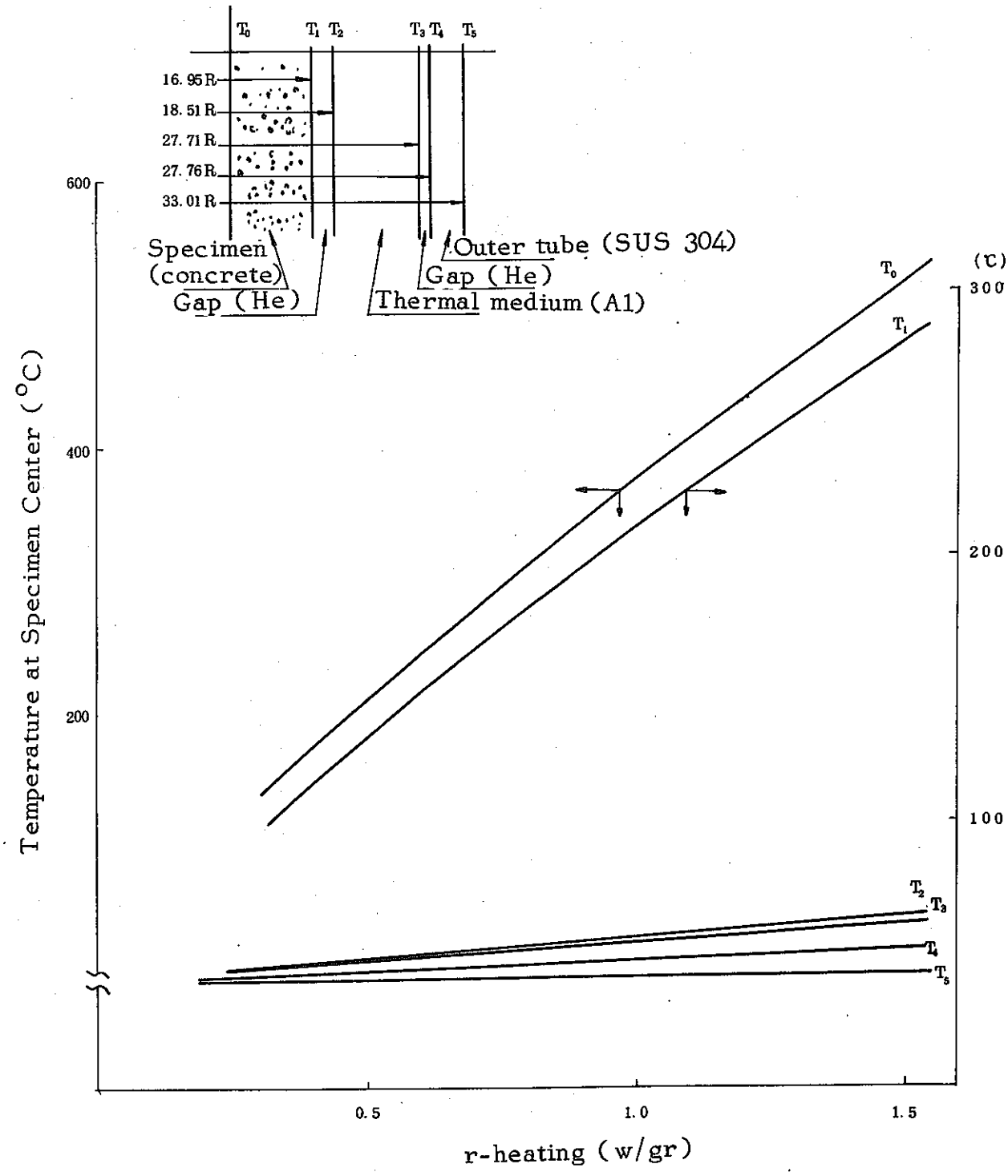

Fig. 5 Temperature Distribution in Capsule for JMTR-SH(I)
(Position of T/C #3)

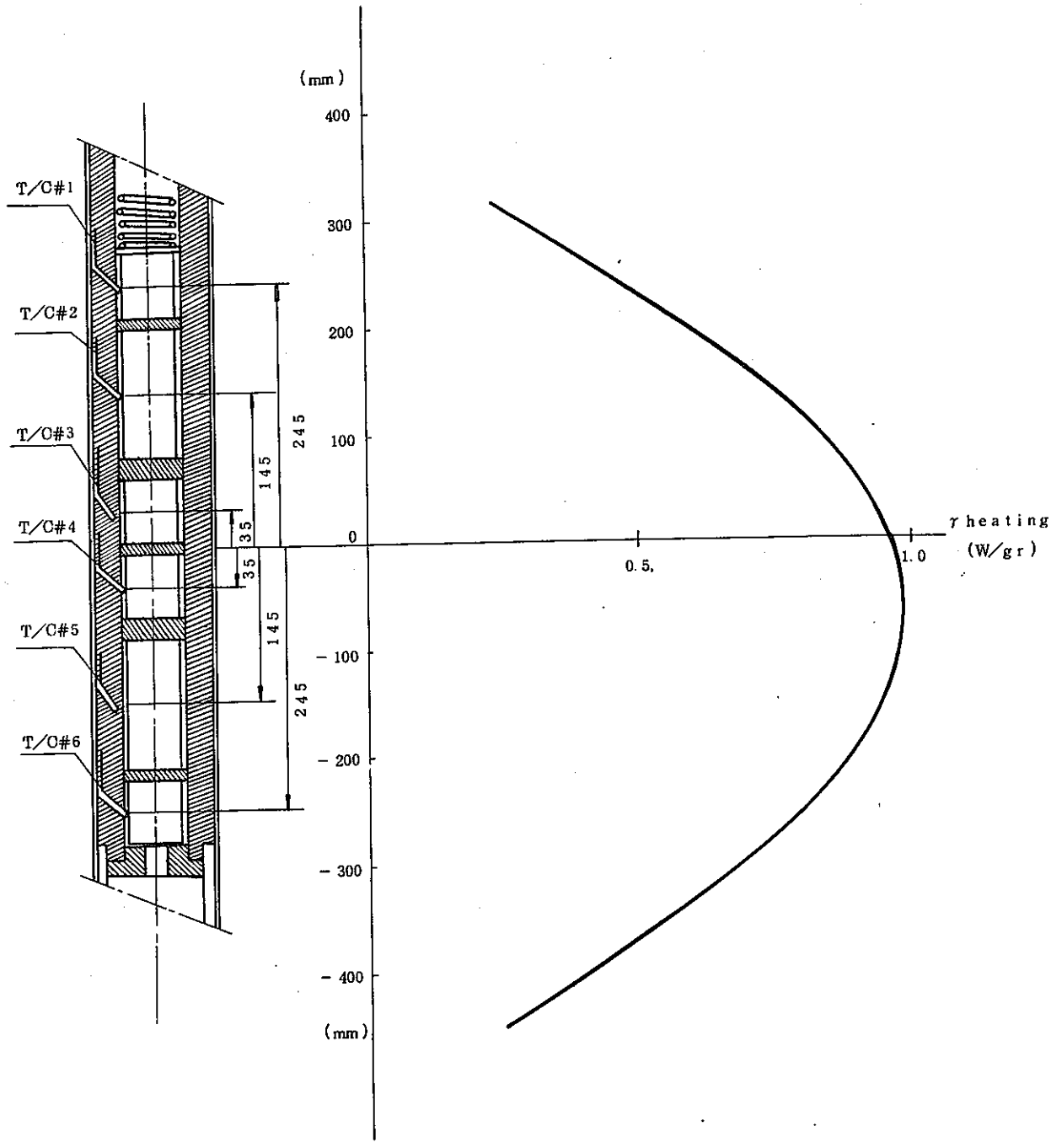

Fig. 6 Relative r-Heating Coefficient in Capsule for JMTR-SH(I)

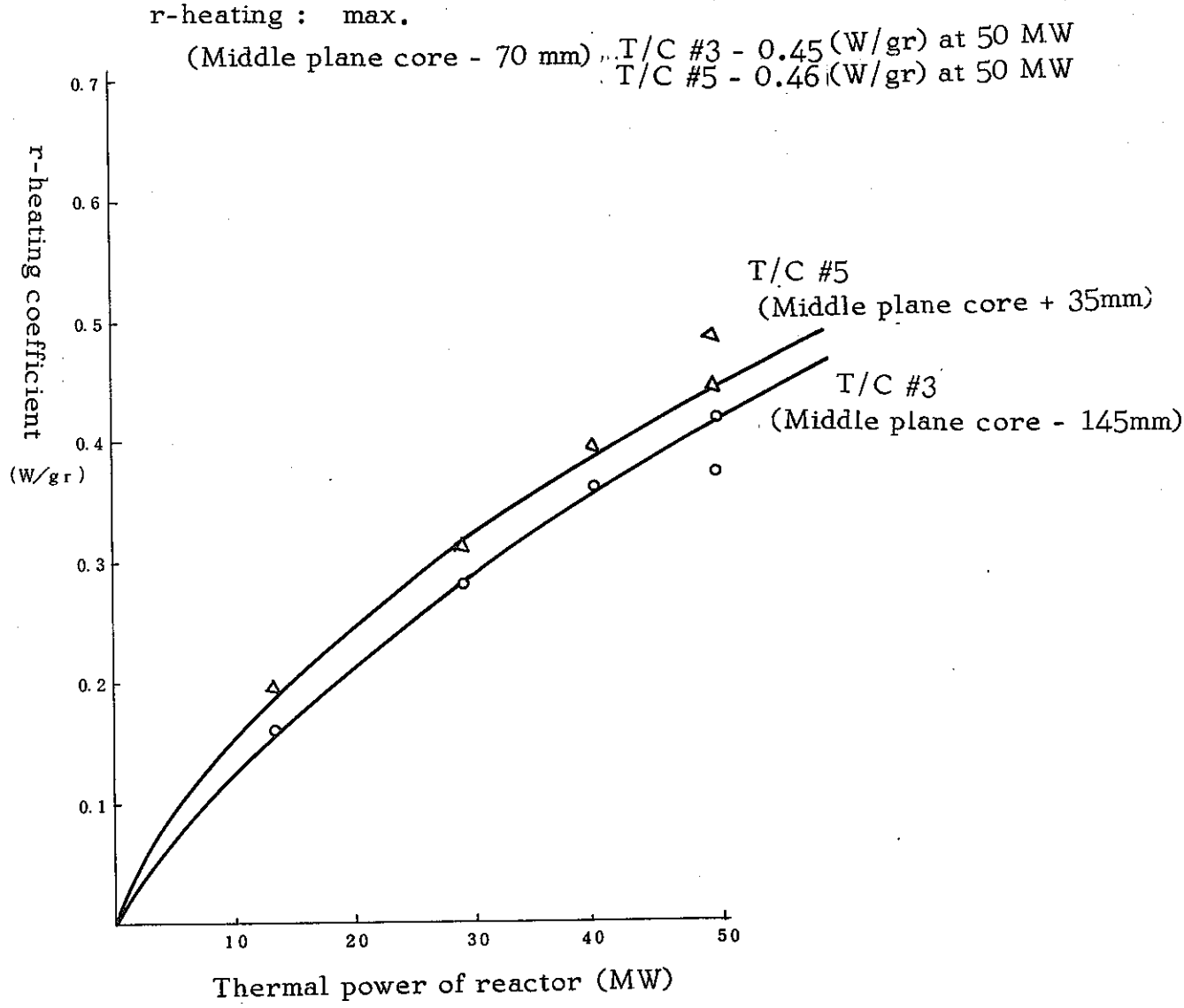

Fig. 7 Relation between Reactor Power and r-Heating Coefficient

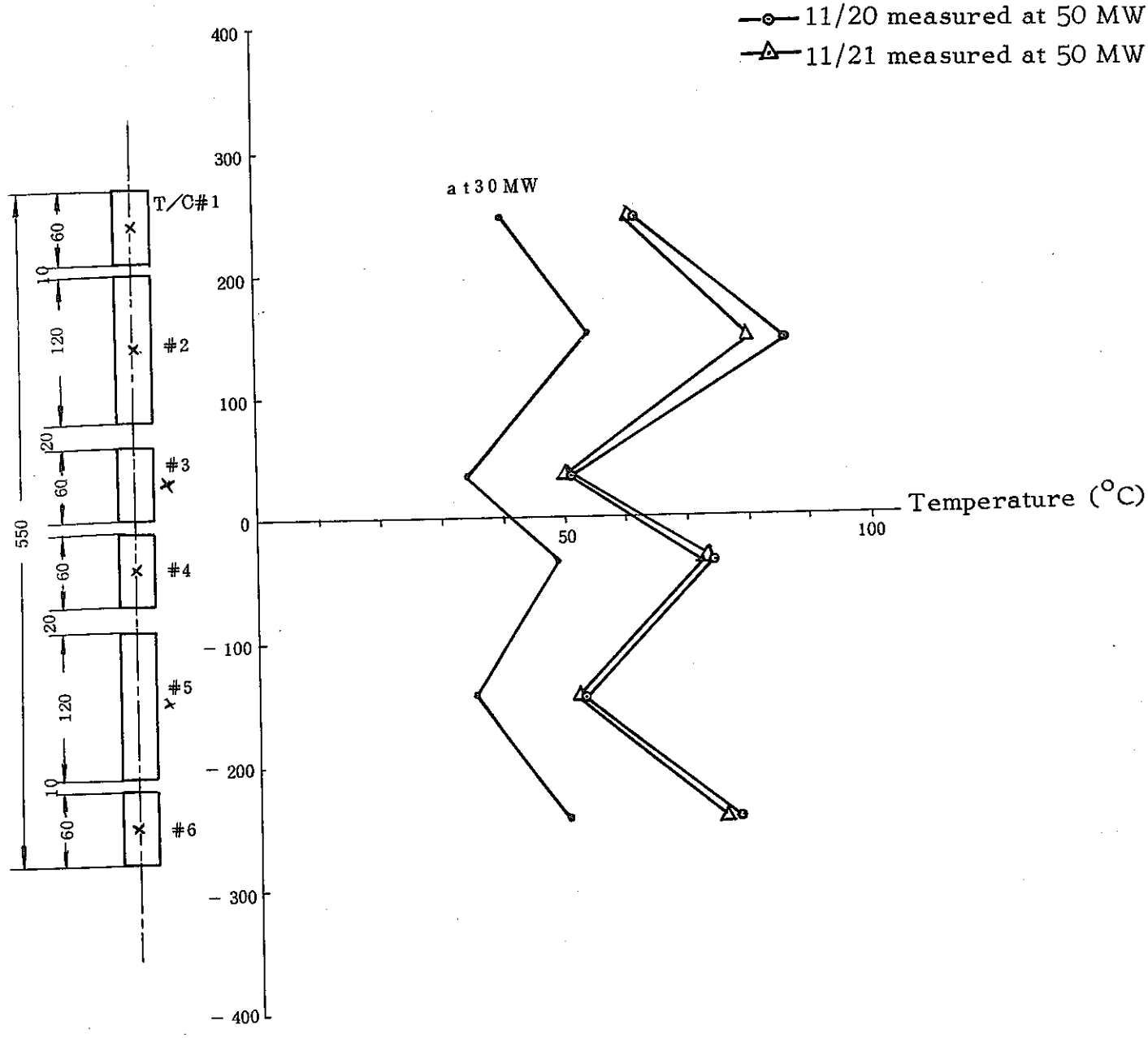

Remarks: As for #3 and #5 thermocouple, temperature in the aluminium medium, and as for #1, #2, #4 and #6 thermocouple, temperature of the surface of specimen was measured.

Fig. 8 Temperature in Capsule for JMTR-SH(I)